

Design, Make & Test Project:

# Final Report

Mechanomyographic-controlled prosthetic hand

[REDACTED]

---

Group 19

Supervisor: Dr Ravi Vaidyanathan

[REDACTED]

Charles Jones

---



## EXECUTIVE SUMMARY

Transradial (below elbow) amputation can be a debilitating condition, making many tasks associated with daily life considerably more difficult for amputees. Prosthetic hands aim to mitigate this issue by providing amputees with a device which can assist in performing complex functions such as grasping objects. However, the limiting factor in upper body prosthetic design has long been the shortfall in control systems, preventing amputees from controlling complex machines such as fully articulated prosthetic hands. Modern solutions to this problem primarily involve using electromyographic (EMG) sensing to pick up on intentional muscle signals and control the device, although this method has considerable disadvantages such as perspiration and sensor placement affecting the results. Moreover, EMG solutions on the market today start at a prohibitively expensive price point of around £ 10,000. This design, make and test project introduces ATLAS, a novel solution using mechanomyographic (MMG) muscle sensing to control the device (shown in Figure 1). The prosthetic hand can form three user-controlled grip poses (point, grasp, and open), controlled through a specially designed MMG-sensing armband which was demonstrated to produce up to 90 % muscle sensing accuracy when tested virtually with a dataset of 17 labelled muscle movements over 6 different muscles. The mechanical design of ATLAS draws from fields such as soft robotics and biomimetic design, using a composite structure that enables grasping of a variety of hard, soft and irregularly shaped items with robust functionality: in testing, ATLAS was able to pick up objects of over 3.5 kg with ease. ATLAS is fully 3-D printable and can be manufactured for under £240, lending itself to an open-source, distributed manufacture model of production, specifically intended to be of most benefit to amputees in developing countries and children. Unfortunately, the unprecedented coronavirus outbreak cut short the practical time available for this project, however, all possible steps were taken to mitigate this effect and an alternative work package was completed to ensure the project remained of high quality despite these setbacks.



*Figure 1: ATLAS (without electronics or sensors)*



## CONTENTS

Executive Summary .....	ii
Contents .....	iii
Acknowledgements .....	iv
1 Introduction .....	1
1.1 Brief .....	1
1.2 Team Roles .....	1
1.3 Report Structure .....	2
2 Literature Review and project background .....	3
2.1 Transradial amputations and needs of amputees .....	3
2.2 Principles and paradigms of upper body prostheses .....	3
2.3 Mechanomyographic techniques for muscle sensing .....	5
3 Design .....	7
3.1 Product Design Specification .....	7
3.2 Expert Research Meetings .....	9
3.3 Conceptual Design .....	10
3.4 Mechanical Design .....	14
3.5 Control Design .....	23
3.6 Electronic Design .....	31
3.7 Final Design .....	36
4 Manufacture and Assembly .....	37
4.1 Methods and Justification .....	37
4.2 Mechanical characteristics of FDM printed parts .....	38
4.3 Design for 3-D Printing .....	38
4.4 Printing with PETG, PLA and TPU .....	42
4.5 Assembly of electronics .....	43
4.6 Overall assembly .....	43
5 Product Cost and Budget .....	45
5.1 Finance and budgets .....	45
5.2 Final Product Cost .....	45
6 Testing and Design Verification .....	47
6.1 Destructive Testing .....	47
6.2 Grip Strength Test .....	50
6.3 User Testing .....	51
7 Alternative Work Package .....	52
7.1 Effect of early university shutdown on project .....	52
7.2 Details of uncompleted tasks .....	52



7.3	Details of alternative work package.....	53
7.4	Alternative Work .....	53
8	Discussion .....	59
8.1	PDS Evaluation .....	59
8.2	General Discussion .....	61
8.3	Future Work .....	64
9	Conclusions.....	65
10	Personal Reflective Reviews.....	66
10.1	.....	66
10.2	.....	66
10.3	.....	67
10.4	.....	68
11	References .....	70

## ACKNOWLEDGEMENTS

The group would like to extend our warm thanks to the following people and companies:

- ~ Dr Ravi Vaidyanathan for his continuous support throughout the project.
- ~ SERG Technologies for lending us three proprietary MMG sensors.
- ~ Alex Lewis for his invaluable advice and input.
- ~ Liang He for taking the time to discuss his research on soft robotic actuators.
- ~ Vim Patel for his oversight and help in the electronics lab.
- ~ Aslan Kutlay for his input on constructing the demonstration stand



## 1 INTRODUCTION

### 1.1 BRIEF

Today's market for upper body prosthetics is broadly divided into high-cost, high sophistication, electro-mechanical designs, and low-cost body-powered devices with less functionality (elaborated upon in the literature review, section 2). This project aims to bring the advantages of electromechanical prostheses to consumers at a significantly lower price point by exploiting two emerging techniques: mechanomyographic (MMG) muscle sensing and open source distributed manufacturing. At the beginning of the project, the following five targets were set out:

- ⚡ Design and manufacture a prosthetic hand capable of forming multiple useful grip patterns.
- ⚡ Design a comfortable strap to house muscle sensors and a basic socket to suspend the device from a demonstration stand.
- ⚡ Sense and analyse MMG muscle signals, producing an algorithm to accurately classify muscle contractions.
- ⚡ Implement a control system so the user can accurately move between the grip patterns by utilising intentional muscle movements.
- ⚡ The final product must be manufacturable by volunteer engineers or hobbyists at a low price.




These ambitious targets are designed to enable the creation of a new class of prosthetic device – one which can bring the functionality associated with high-cost prostheses but be open-sourced and manufactured at a low cost by amputees themselves or volunteers.

### 1.2 TEAM ROLES

Although all members of the team contributed to many aspects of the project, and supported each other wherever necessary, a summary of primary roles are listed below, together with the headline requirements and responsibilities of the role. Team members had a management role which supported the organisation of the team and project, as well as a technical role. These were allocated based on previous project experience, areas team members wanted to focus on, and ME1/2/3 module experience, and are listed below in Table 1.



Table 1: Team roles and responsibilities

<b>Name</b>	<b>Management Role</b>	<b>Technical Role</b>
	<b>Project Manager</b> Ultimately responsible for ensuring all elements of the project progress on track and to a suitable standard, in line with internal and external deadlines, and allocating resources to ensure that deadlines are met.	<b>Electrical Lead</b> Lead for the design, testing, build and assembly of physical electronics.
	<b>Meeting Coordinator</b> In charge of organising group meetings and room bookings.	<b>Manufacturing Lead</b> Responsible for manufacture and printing, and also for providing input on design for additive manufacturing to the mechanical design process.
	<b>Procurement + Finance Lead</b> Responsible for managing, facilitating and approving purchase requests (together with the PM), and ensuring expenditure remains within budget and restrained.	<b>Mechanical Design Lead</b> Lead on design process, bringing together work from other team members regarding product design from inception right through to final prototype stage.
Charles Jones	<b>Document Lead</b> In control of overall document management, including Quality Plan, Progress Report and Final Report, and creating timelines to ensure these are produced on time.	<b>Coding Lead</b> Responsible for all software elements of the design, from signal acquisition and processing to digital user experience design.

### 1.3 REPORT STRUCTURE

This report aims to present the final product, ATLAS, and the care and attention invested into all three areas of design, make and test. It begins with a literature review, outlining the market need for a product of this type, the background of the market, and consideration of different prosthetic control methods. Section 3 addresses the design progression, covering the full process from conception to detailed design of the mechanical, electrical and control systems of the device. It is important to note that ATLAS was explicitly designed using a continuous, iterative cycle of prototyping and testing, so this section includes many of the tests which were performed to inform design decisions. Section 4 details the manufacture of the product, explaining the methods and materials chosen, alongside considerations made when designing with these in mind. Section 6 then documents the testing performed to verify design decisions, refine areas of the product and to evaluate if the product performs as specified. This project was unusual in that it was interrupted by a complete shutdown of practical university work in response to the unfolding pandemic COVID-19, so a section was included to discuss the effects of the shutdown on the project and provide alternative work to replace the work that was cut short. The discussion and conclusions follow, and the report finishes with personal testimonials from each of the four group members



## 2 LITERATURE REVIEW AND PROJECT BACKGROUND

A literature review was conducted to understand modern prosthetic devices and the market for them today – first, the prevalence of transradial (below elbow) amputations and the needs of amputees were established and the principles and challenges of modern prosthetic design were examined. Finally, the review covers the emergence of mechanomyography (MMG), a novel muscle sensing technology which is used to control the ATLAS prosthetic hand made by this group.

### 2.1 TRANSRADIAL AMPUTATIONS AND NEEDS OF AMPUTEES

The dexterity of the human hand to perform complex mechanical tasks possesses no parallel in the human body; it is often modelled as a machine with 27 independent degrees of freedom (1) and it has huge versatility – giving it uses in all areas of modern life, including sports, personal care, cooking, communication and more. The loss of a hand from a transradial amputation is an extremely debilitating condition which typically occurs after a traumatic injury (2), and maximising quality of life after such an injury is best achieved through a program of rehabilitation utilising prosthetic devices to allow the patient to re-learn daily tasks (3). The needs of prosthetic device users are well known, with studies over the previous 20 years (4,5) corroborating the same few key desires: the ability to perform tasks such as dressing and eating with knife and fork; anthropomorphic aesthetics; reliable, high strength grasping with their prosthesis; and comfort using the device.

### 2.2 PRINCIPLES AND PARADIGMS OF UPPER BODY PROSTHESES

Mechanical design of fully articulated, anthropomorphic hands is, in principle, straightforward. These devices exist in robotics development (reviewed in (6)). However, prosthetic devices have yet to match the ability for independent finger articulation of these robots. This is in large part due to control systems and the interface between the user and the machine lacking the necessary complexity to allow control in all 27 degrees of freedom. The two main control methods used in prosthetic devices on the market today are body-powered control and electromyographic (EMG) control.

Body-powered prostheses rely on the user providing the power and control of movement by physically actuating the device's mechanism (often using a harness and tension cable system which the user pushes against). The most common type of body-powered prosthetic device is the split hook, depicted in Figure 2(A) – these provide a durable solution which give the amputee the ability to perform simple grasping movements. Unfortunately, however, their functionality does not extend much further than that, which is a key reason why many amputees abandon their prostheses



entirely. As many as 56 % of upper limb amputees wear their prosthetic limb ‘once in a while’ or ‘never’ and 64 % of amputees rate the functionality of them as ‘fair’ or ‘not acceptable’ (7) – this high rejection rate, combined with the poor aesthetics of split hooks, has meant they have begun to fall out of favour in recent years.

Electromyographic-controlled prostheses (also known as myoelectric or EMG), depicted in Figure 2(B), are a more modern solution and typically show lower rates of user rejection than body-powered prostheses (8). These devices allow the user to control an electronically powered prosthetic hand by using voluntary muscle contractions that are picked up by electrodes, which can be placed on the surface of the skin, as reviewed in (9), or implanted into the user’s forearm muscles (as in (10)). These devices typically have several pre-programmed grip patterns which the user can move between, giving them superior functionality to body-powered prostheses. Arguably the most significant issue with the myoelectric prostheses available on the market today is their prohibitively high price point, typically of the order of £10,000 and upwards – naturally, this has spurred significant research interest in developing low-cost alternatives to these products (11-13), however, none of these lower-cost products have yet proven to be viable as a long-term solution for amputees.

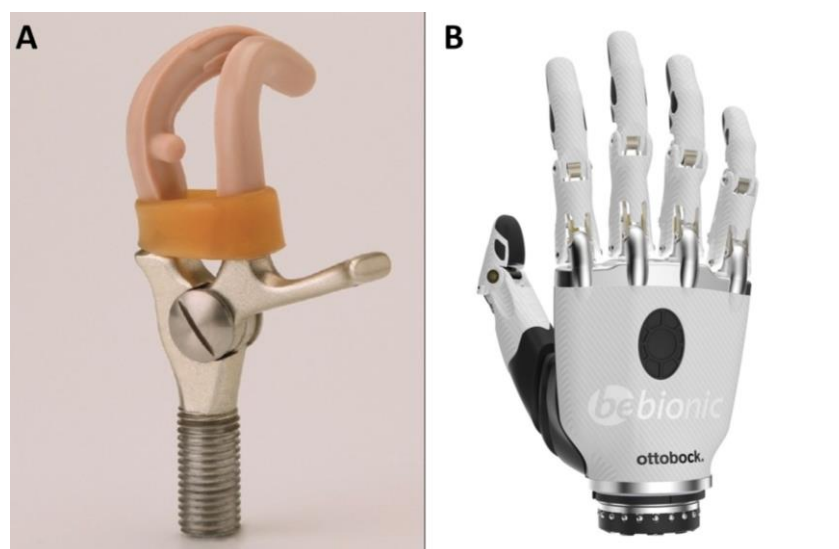


*Figure 2: Body-powered split hook prosthesis (A), adapted from figure 2 of (14). Ottobock BeBionic myoelectric prosthesis (B), figure from ottobockus.com (15).*

Thus, amputees are today faced with a difficult choice when selecting between devices – either choose a mechanical device with high reliability but limited functionality or have to part with potentially tens of thousands of pounds for a myoelectric device. This problem is exacerbated when considering that many countries do not have health services that will purchase these devices for





amputees; moreover, children are often denied expensive devices because the investment is too great for a product which they will grow out of in a couple of years. A brief comparison of several notable myoelectric products, and a well-known open-source mechanical design, are presented below in Table 2, illustrating the wide range of price-points and functionality.

*Table 2: Comparison of variety of products on the market*

<b>Product, [Manufacturer]</b>	<b>Cost</b>	<b>Product information</b>
<b>Michelangelo hand [OttoBock]</b>	£ 46,000	Aesthetically pleasing design with a silicone glove for added realism. Hand can perform 7 pre-set grips and models the action of bones and joints.
<b>Bebionic [OttoBock]</b>	£9,000	The hand is capable of 14 grip patterns, with actuation on each individual digit, and an adjustable hand position.
<b>Hero Arm [Open Bionics]</b>	£5,000	This is the cheapest myoelectric device on the market, in part due to its 3-D printed design. However, it has not yet been approved by the NHS in the UK.
<b>Phoenix Hand [E-NABLE]</b>	£50	A 3-D printed, open source, body-powered design. Low functionality and low durability.

One further challenge of prosthesis design is the suspension of the device from the amputee. Modern devices typically use one of three techniques for prosthesis suspension: self-suspended, suction methods, and harness methods. The advantages and disadvantages of each method are discussed in (16) and (17) provides a review on the topic of prosthetic interface and its effect on comfort. This area of prosthetic design, however, is not the focus of this DMT project, so will not be discussed any further in this review.

## 2.3 MECHANOMYOGRAPHIC TECHNIQUES FOR MUSCLE SENSING

One alternative to the paradigms of body-powered and EMG prostheses that has gained traction in recent years is mechanomyographic-controlled (MMG) prosthetics. MMG muscle sensing relies on sensing low-frequency, mechanical vibrations generated by muscles during a voluntary contraction and has been shown to produce comparable results to traditional EMG sensing (18-20). Although EMG is typically considered the gold standard for muscle sensing, MMG methods have several



practical advantages that suit use in a prosthetic hand, including low sensitivity to changes in skin impedance and low sensitivity to non-optimal sensor placement – both of which are well-known problems with EMG sensing (21,22). The nature of MMG signals as vibrations also means that the hardware requirements for MMG sensing are simple and low-cost, requiring only microphones with no amplification necessary.

Despite these advantages, there have been relatively few attempts to develop a prosthetic hand controlled by these signals, with notable research coming from Imperial College London's Biomechatronics laboratory (23,24). A spin-off company from Imperial, *SERG technologies*, has recently begun development into this very field, so it is the authors' hope that commercial MMG-controlled prosthetics will become available in the coming years.



### 3 DESIGN

The first major step in the engineering process was the actual design of the product. Initially, quantifiable targets for the project were set out in the PDS. From there, concepts were developed, and a morphological analysis conducted upon the different aspects of the concepts. The design was then split into mechanical, electrical and control streams; each being designed largely in parallel with all sections coming together in the final design.

#### 3.1 PRODUCT DESIGN SPECIFICATION

The first stage of the design process involved constructing a product design specification (PDS), shown in Table 3. This was produced from the targets set out in the brief (section 1.1), using insight gained from the literature review (section 2); the PDS sets out quantitative objectives that the product can be designed for and tested against to ensure high quality through the design, make and test process. Naturally, due to the number of unknowns at the beginning of the project, the PDS was refined several times due to increased knowledge about the technical aspects of the project, a topic elaborated upon in the project progress report and quality plan documents (25,26). Aspects which were subject to change are marked with an asterisk and the history and reasons for the change are more fully explained in the progress report.

Some aspects of the PDS are crucial for successful delivery of the project targets, whereas other aspects are less important either because they do not affect the project as much or because the objective was chosen as an arbitrary target. To create a clear demarcation between these three levels of importance, the aspect section of the PDS was color coded, with green aspects being crucial to the project performance, yellow aspects being important, but arbitrarily chosen goals and blue aspects being non-critical to the delivery of the final product.



Table 3: Product Design Specification

	Aspect	Objective	Justification	Verification
Performance	Number of grip poses*	$\geq 3$	Three poses should provide sufficient functionality for key uses in daily life.	Design review.
	Maximum grip force	$\geq 30$ N	30 N is suitable for basic daily tasks such as carrying shopping and shaking hands.	Prototype testing using force meter.
	Sensing method	MMG	MMG sensing will be used for signal acquisition.	Design review.
	Gesture recognition accuracy	90 %	For the device to be useable daily, it must correctly actuate 90 % of the time to avoid user frustration.	Prototype testing.
	Battery life	12 hours	12 hours of continuous use would last through a full workday and use at home.	Prototype testing.
Life	Product lifespan	2 years	Operate for a minimum of 2 years before failure under standard use.	Fatigue testing of prototype.
	Waterproofing	IP33 rating	This should allow for protection from splashes and small solid objects.	Test prototype against standards.
Size	Form factor	Adult sized right hand	The device should fit adult transradial amputees. A basic socket will also be designed for demonstration purposes, although this is not the focus of this project.	Design review.
	Mass	< 500g	An average human hand has a mass of approximately 500g. This should therefore be a reasonable upper limit for the product mass, to avoid user discomfort.	Weigh prototype with digital balance.
Safety	Maximum electronics temperature	< 40 °C	Skin-contact and external surface temperatures must remain under 40 °C to avoid potential discomfort and burns (based on ASTM C1055 standards (27)).	Run for 10 mins then scan with infrared thermometer.
	Transmission enclosure	Enclosed	Transmission parts should be enclosed for the user's safety.	Design review.
	Electronics enclosure	Enclosed	Electronics should be enclosed to minimise the chances of burns and shocks.	Design review.
	Loading	$\geq 50$ N	The mechanism must not break when overloaded.	Perform loading test on prototype.
Production	Quantity	$\geq 2$	An initial working prototype will be made followed by a final product.	Count prototypes.
	Cost*	< £400	If the final device has a materials cost of less than £400, it will be accessible to users with a wide range of economic circumstances.	Summing cost from bill of materials.
	Materials*	Cheap and widely available materials	Material selection will occur at a later project stage and will be intertwined with the manufacturing processes chosen.	Design review.
	Processes	3-D printing and related methods	The product must be manufacturable by volunteer hobbyists and engineers using methods reasonably accessible to them.	Design review.
	Assembly	< 3 hours	Must be assembled and fitted to an amputee in less than three hours by an engineer.	Timed test with stopwatch.
	Training	<30 mins	New users should be able to learn the basics of controlling the system quickly to avoid frustration.	Timed test with stopwatch.



## 3.2 EXPERT RESEARCH MEETINGS

Early in the design process, we decided to organise meetings with experts in fields relevant to this project. Fortunately, both Alex Lewis and Liang He kindly offered us their time and meetings with them yielded some extremely valuable insights into different areas of the design. The first meeting was with Alex Lewis, a quadruple amputee who sits on the board of directors of SERG technologies (a spin off company from Imperial focussing on the uses of mechanomyography). Liang He, who we met in the second meeting, is a soft robotics PhD student from Imperial's Dyson school of Design Engineering.

---

### 3.2.1 MEETING WITH ALEX LEWIS

The key insights from the meeting with Alex were:

- ⚡ He had found that the robustness and versatility of non-mechanical prosthetics is a major issue; for day-to-day use, he uses a mechanical split-hook.
- ⚡ Having a prosthetic capable of multiple, simple day-to-day tasks would be beneficial. Examples he gave included: picking up a glass, moving a variety of objects around, or holding cutlery.
- ⚡ In his opinion, the performance of a prosthetic is far more important than how it looked; he believed that this opinion was held by most amputees, including children as well as adults.

---

### 3.2.2 MEETING WITH LIANG HE

The aim of the meeting with Liang He was to gain more of an insight into how soft robotics like those used in medical procedures could influence a prosthetic design. The key insight was that for an electromechanically controlled prosthetic, the stiffness of the composite finger design is a major design variable and would need careful consideration. He also discussed haptic feedback, and the various methods that could be delivered (through mechanical vibration, sound, or electrical stimulation), but noted this could be a complex addition to the project. It was also noted that electrical or mechanical stimulation near the MMG sensors could cause significant interference.



### 3.3 CONCEPTUAL DESIGN

During conceptual design, it is important to generate a wide range of ideas, taking many forms and using different mechanisms and technologies to solve the same problems. This section details the process followed when considering different concepts and ideas, using a morphological chart to aid decision making and produce a final concept.

#### 3.3.1 IDEATION

Figure 3 displays some early stage annotated ideas, which were then developed into the first concepts. Some key considerations are how many digits the hand has, how the digits are actuated and the grasping mechanism.

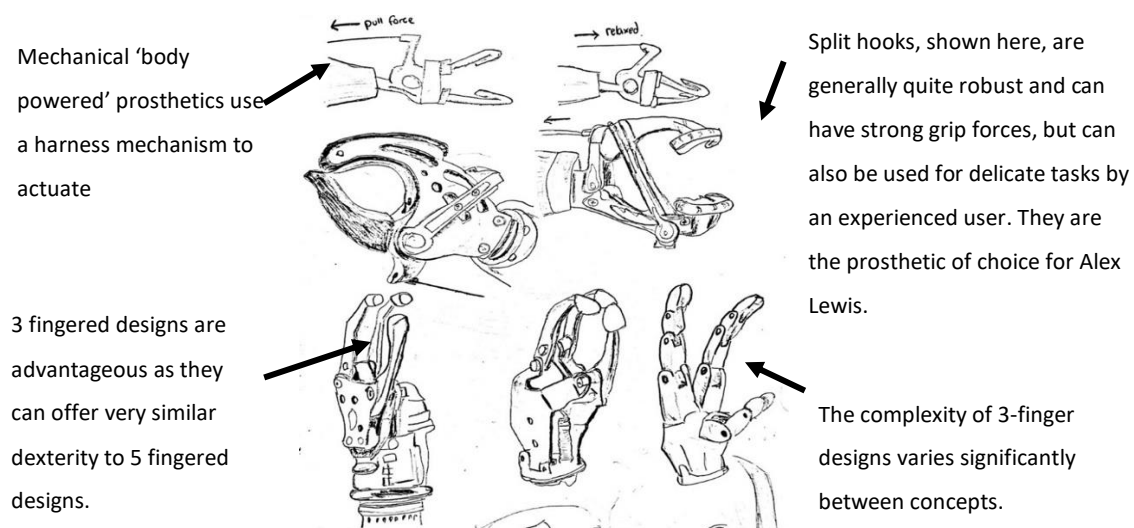


Figure 3: Selection of initial ideas

#### 3.3.2 INITIAL CONCEPTS

This section introduces 3 of the most interesting concepts produced in this process. These were influential in constructing the morphological chart, which includes aspects from each of these concepts and more.

The first concept, shown in Figure 4, is a design with 5 digits. The 4 fingers are connected to a linear motor with tendons and the force is distributed equally across them using a 'whippletree' mechanism. The thumb is actuated by a separate linear motor on the underside of the hand and the fingers have a design of 3 phalanges per digit (meaning 3 independently articulated sections). The benefit of this design is that by having only two motors, the cost for electronics would be low;



however, the drawback would be that there is less scope for different poses, as the four fingers cannot be actuated independently.

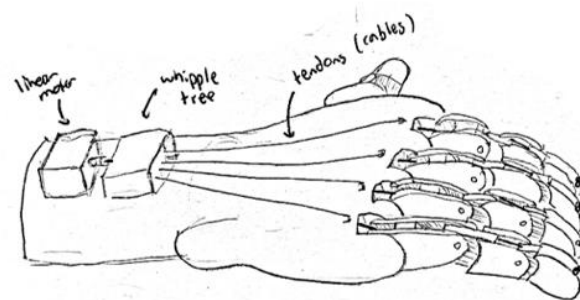


Figure 4: Concept 1

Figure 5 shows a second 5-digit concept. Each finger has two phalanges, which are actuated by a DC motor using worm gears and linkages. The design also contains a rotating wrist, and a pivoting thumb. The main benefit of this design would be the scope for many different grip poses, and the dexterity that would provide. However, the drawback would be that the design is quite complex mechanically and electronically, and thus likely quite expensive and difficult to manufacture.

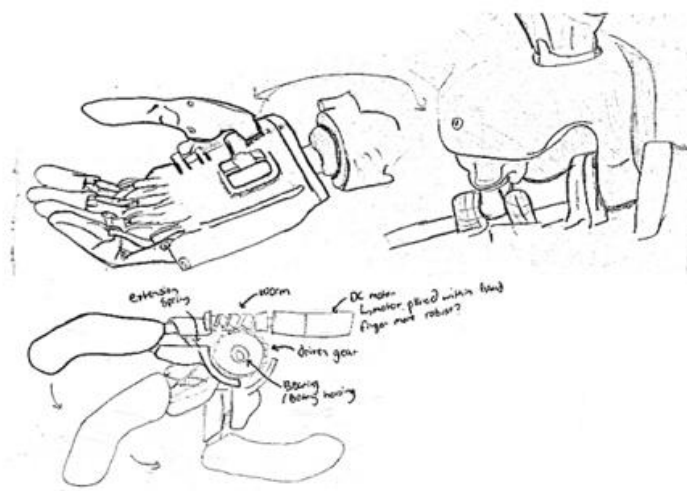


Figure 5: Concept 2

The third concept (Figure 6) is focussed on the digits themselves. In this concept, the fingers are based off human biology, where hard bones lend rigidity and a soft outer skin gives grip and durability. The advantages of this approach are self-evident as the concept could, in theory, come



the closest to matching the capabilities of human fingers. There is, however, increased design complexity and care would be necessary to tune the ratios of hard and soft material.



Figure 6: Concept 3

### 3.3.3 MORPHOLOGICAL ANALYSIS

After the initial conceptual design, a morphological analysis was conducted to identify the many possible variations of the key features of the product. This involved splitting the prosthesis into sub-features and design elements, and listing various concepts proposed to meet them. Using a ranking and weighting technique, the most suitable concept was selected for each aspect. Some features, such as haptic feedback, were decided as potentially unrealistic with the time and resources available and it was agreed to put them on hold, only considering their addition if significant time opened up later in the project. Table 4 displays the morphological chart produced, with the selected concepts highlighted in green and a qualitative explanation of the key design decisions is below.

Table 4: Morphological chart for overall design

Sub-feature	Concept 1	Concept 2	Concept 3	Concept 4
<b>Grip Type (No. of digits)</b>	5	3	Split hook	Mitten
<b>Digit characteristic</b>	Hard / Stiff	Soft	Compound	
<b>Actuation</b>	Tendon	Linkage / Pushrod	Gears	
<b>Motor Type</b>	Linear	Rotary	Stepper	Electromagnets
<b>No. of phalanges</b>	1	2	3	4
<b>Socket design</b>	Forming	Foam and Straps	Airbag	





Thumb – Degrees of Freedom	1 DOF	2 DOF	Fixed (0 DOF)	
Wrist Rotation	Yes	No		
Feedback	None	Haptic	Electric	Auditory

- ✦ **Grip type:** it was clear from the meeting with Alex Lewis that function is more important than form, therefore a 3-finger design was chosen for the final concept to reduce design complexity whilst maintaining function.
- ✦ **Digit characteristic:** Having a composite biomimetic design of hard ‘bones’ and soft ‘skin’ was deemed an exciting and effective avenue for development.
- ✦ **Actuation:** A simple but robust design of linear motors driving tendon cables was decided.
- ✦ **Number of phalanges:** In keeping with the biomimetic design, 3 phalanges were used. This style allows the fingers to bend into a good shape for grasping objects.
- ✦ **Socket design:** Socket design was not considered to be a key focus of this project, so a simple concept was chosen for use with a display stand.

#### 3.3.4 FINAL CONCEPT

The final concept invoked from the morphological analysis is depicted in Figure 7. This concept involves a hand with three fingers, each with hard and soft components to mimic the human hand. The fingers are actuated using tendon wires driven by linear motors and a simple socket is included for demonstration and testing.

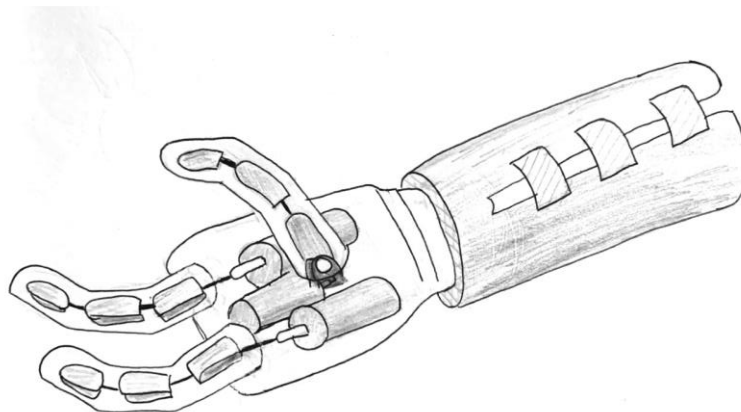


Figure 7 - Final Concept



### 3.4 MECHANICAL DESIGN

This section details the mechanical design of the product and the reasoning, iteration and calculations involved in this process. A philosophy of rapid prototyping using 3-D printing was used, allowing small design, make and test cycles to drive iteration and improvement. The ambitious nature of our PDS made calculation and logical reasoning crucial to the design process.

---

#### 3.4.1 MATERIAL SELECTION

When designing the product, material selection was an important parameter, considered from the very start of the process. One of the aims of this project set out in the brief is for the final product to be manufacturable by a volunteer hobbyist or engineer – so the main manufacturing method chosen was 3-D printing (explained in full in section 4.1).

There are three main groups of filaments for printers: standard solid filaments; flexible filaments; and exotic particulate filaments. A standard solid filament is a filament which is made from one main plastic and occasionally a bonding agent. They can usually extend by up to around 25 % before fast brittle fracture occurs. A flexible filament is the same as the solid filament in the sense that it is one main plastic, however it has a maximum elongation above 400% before failure. So-called ‘exotic particulate’ filaments are a mix of a plastic with a filler, for example wood fibres or graphite, which add properties such as electrical conductivity or increased strength. Although creating a material with electrical conductivity would mean the electrical connections could be printed directly into the parts, this would require a dual extrusion printer (to produce the conductive / not-conductive sections in parallel) which goes outside of our PDS, as dual-extrusion is not a common entry-level 3-D Printer.

There were three material selections that needed to be made. They are listed below, along with the requirements:

- ✦ Socket – Requirements: mouldable at relatively low temperatures (achievable without specialist equipment), but not so low that the form could change under normal use, relatively tough, relatively light.
- ✦ Outer finger ‘skin’ – Requirements: flexible with high durability and toughness
- ✦ Rest of product – Requirements: hard, low-density, tough (retaining these characteristics within the expected operating temperature range).



After some research, we decided to use three different materials: Polylactic Acid (PLA) for the socket; Thermoplastic Polyurethane (TPU) for the fingers; and Polyethylene Terephthalate Glycol (PETG) for the rest of the product. A summary of the properties of each of these plastics can be seen below in Table 5. These properties are for a homogenous piece and will not quite reflect the properties of a fused-deposition product. Thus, as part of the design validation process, the actual strength of our parts was tested, as can be seen in section 4.3.1 and section 6.1.

*Table 5: Summary of PLA, PETG & TPU Material Properties. Values taken from (28).*

	PLA	PETG	TPU
<b>General Classification</b>	Standard solid filament		Flexible Filament
<b>Density (g/cm<sup>3</sup>)</b>	1.29	1.28	1.21
<b>UTS (MPa)</b>	46.8	48	38.1
<b>Elongation at Break (%)</b>	62.9	59	549
<b>Young's Modulus (GPa)</b>	2.8	2.83	0.147
<b>Print Temperature (°C)</b>	180	250	200
<b>Softening Temperature (°C)</b>	71.7	92	105
<b>Glass Transition Temperature (°C)</b>	52.6	83	-21.8
<b>Average Cost per Kilogram (£)</b>	20	25	25

### 3.4.2 FINGER DESIGN

The use of an iterative design process on the fingers was extremely beneficial. The finger concept was chosen to be a composite design of hard interior 'bones' and soft outer 'skin', actuated by a linear motor which pulls a tendon wire (made from fishing wire). Flexible TPU filament was chosen for the soft skin, with PETG for the hard bones. The stiffness of the fingers is a key design parameter, as they must be able to deform when the tendon wire pulls them, however, be stiff enough to grasp heavy objects. The complex deformations involved with this design made accurate analytical calculation impossible – so prototypes were designed, 3-D printed and tested as part of the iterative design process – a diagram of the changes to the finger design as this process progressed can be seen below in Figure 8.



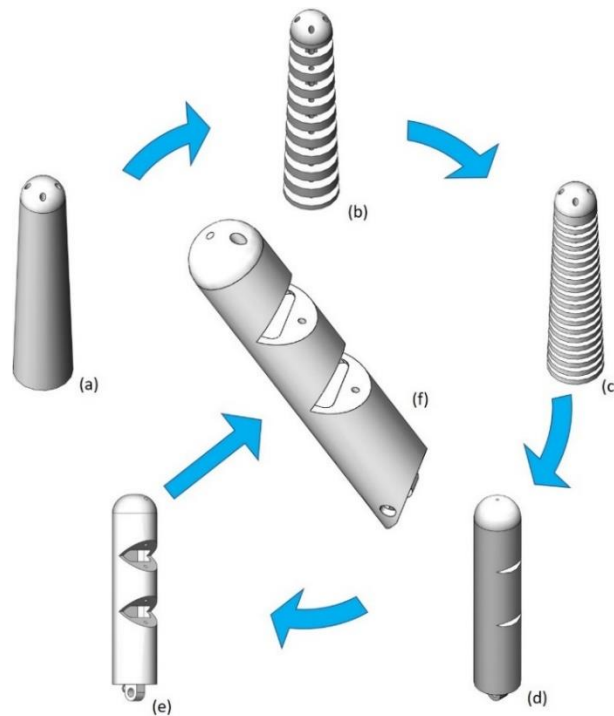


Figure 8: Iterative design of the flexi-finger

- a) The first iteration was a completely solid piece of TPU, with four holes for the threading of fishing wire to control its motion. The design, when printed, was too stiff to bend easily and therefore some material needed to be removed to decrease the second moment of area – explained by Equation 1 which models the initial deformation as buckling of a strut under an off-centre load,  $P_c$ . By reducing the second moment of area, we can thus reduce the necessary force and hence reduce the effective stiffness of the finger.

$$P_c = \frac{\pi^2 EI}{4L^2} \Rightarrow P_c \propto I \quad \text{Equation 1}$$

- b) The second iteration had two types of sections with different second moments of area. One with a smaller second moment of area as it has a smaller cross-sectional area, the rest of the finger has the same cross-sectional area as the first iteration. The finger was easier to bend than the first iteration, however the force required to bend was still too high. One way of adjusting the stiffness of the finger was to vary the infill density of the part. By changing this parameter, an infill of 10% was found to be most suitable.
- c) The third iteration had the same types of sections as the second, however the more of the finger was of the smaller cross-sectional area. This finger suffered the reverse problem of



the previous iterations, with too little stiffness. This iteration struggled to grip objects because it would simply splay out away from them.

- d) This iteration had an internal bone structure which was designed to prevent sideways movement. The wire was routed through the bone structure (based off another prosthetic hand design we had seen). However, there were two main issues with this design. The removed material designed to reduce the second moment of area did not reduce it enough and having the wire inside the bones meant the wire plastically deformed during bending.
- e) This iteration corrected all the issues found in iteration (d) by increasing the cut-out size and moving the wire to attach to the outer flexible part of the finger. This finger worked as desired.
- f) The final iteration had added features for aesthetic and grip improvement purposes. The slope at the bottom makes the whole finger appear flush to the overall hand and a recess was added at the top of the finger to enable a knot in the wire to sit flush with the surface of the finger. The fishing wire is actuated by the linear motor and causes bending due to the force being applied to the tip being off-centre.

---

### 3.4.3 PALM DESIGN

The 'palm' section of the device is important because it contains the electronics, the motors, and the battery. It also provides attachment points for the fingers and influences the mechanics of how the device grasps objects. This was a complex section to design and consists of three parts: a base which houses the motors, provides attachment points for the fingers and channels the tendon cables; a mid-plate which sits over the motors and provides a platform for electronic components; and the cover which simply encloses the structure.

---

#### 3.4.3.1 BASE PLATE

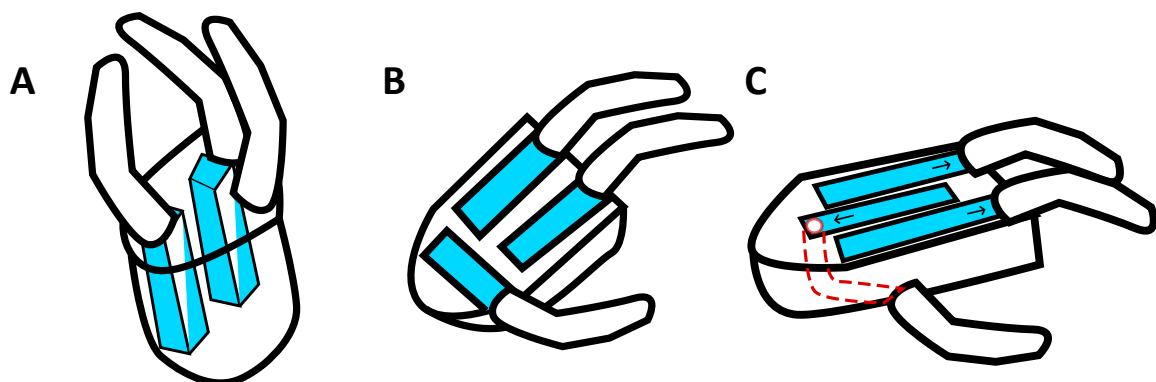
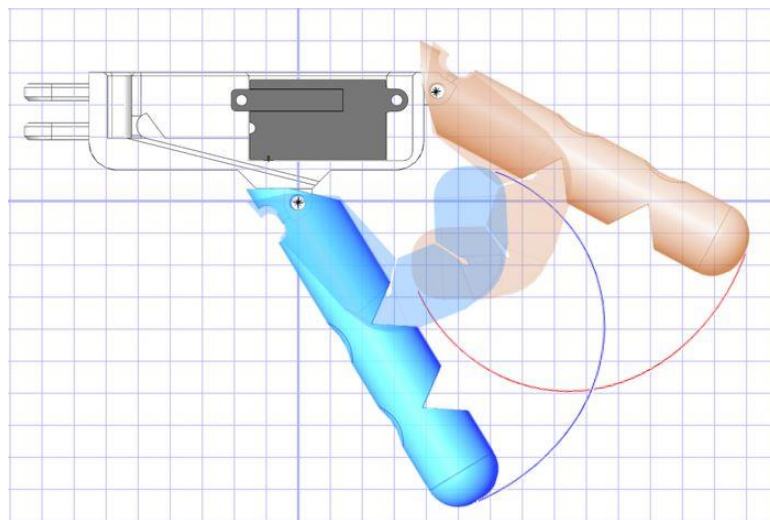


Figure 9 - Concepts for motor placement: (a) face mounted (b) perpendicular mounting (c) parallel mounting



One challenge when designing the base plate was arranging the motors in a space efficient way. Three possible design solutions are shown in Figure 9. (a) Shows face mounted fingers, with the motors held within the base section. The overhang features and the complexity of assembly were the main issues with the proposal. (b) Shows a concept where two fingers come out the top, with the motors in parallel, and the thumb mounted on the side, with the motor perpendicular to the rest. The issues with this design were that it required a large surface area to mount all the motors, and the efficacy of the thumb for gripping was poor. (c) Shows a concept with all three motors parallel with the centre motor in reverse, connected to the thumb on the base of the hand. This was the chosen design as it has the smallest area for all the mounting, with the simplest assembly while maintain a high potential for gripping objects.

Once the motor placement was chosen, the most important design feature was the exact location and spacing of each digit. Through analysing a simplified version of the paths each the finger and thumb would follow, the optimal positioning for grabbing was determined. The path mapping also demonstrates how handles such as those on shopping bags can be grasped easily before being held by the grip.



*Figure 10 - Approximate path of fingers (orange) and thumb (blue)*

Figure 10 shows the path followed by each digit. The end position of the fully flexed digits show that they will form a fully closed overlapping 'clench', a good grip for picking up objects in everyday life as specified in our PDS. Moreover, there is space between the palm and the fingers to hold objects or handles in the fully closed position. This analytical approach was supported by real-world evidence, attained by producing a working prototype (described in full in 3.4.7). The prototype confirmed the efficacy of this finger positioning and allowed some fine tuning of the design when moving to the final version.



---

### 3.4.3.2 MID-PLATE AND COVER

The mid-plate and cover were not designed until after the working prototype was tested. This is because these parts, although important, are largely cosmetic so were not worked on until after the design of the base plate had been experimentally verified to work. The role of the mid-plate and cover is to contain the electronics in a space efficient, aesthetically pleasing package; Figure 11 shows the mid-plate and cover on the final design, with annotations describing the changes made as a result of the working prototype testing:

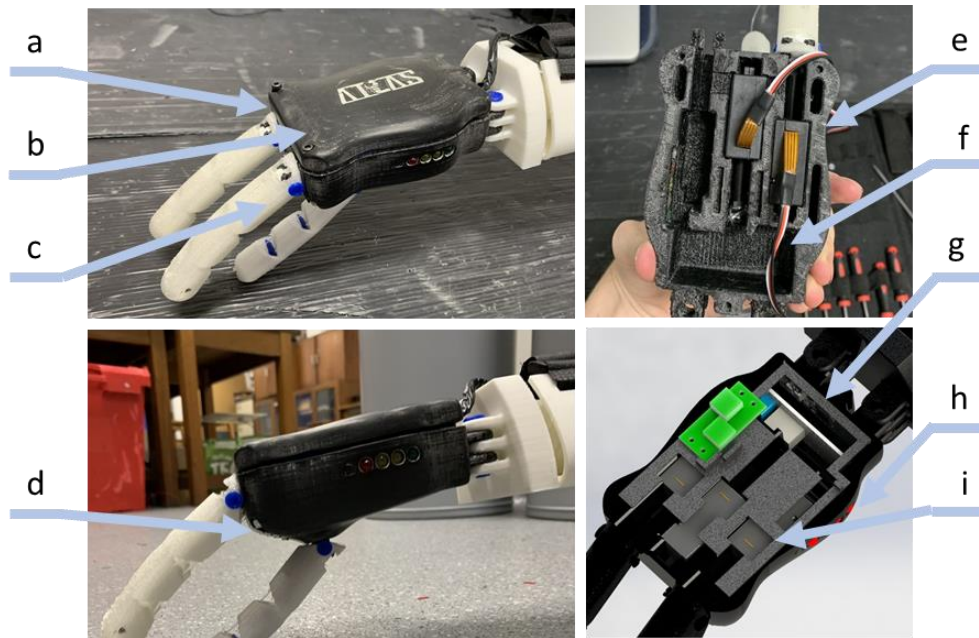


*Figure 11: Final palm design with annotated features*

- a) The sides of the hand section were curved to improve the aesthetics of the device, without minimising structural integrity or function.
- b) Logo imprinted into the cover.
- c) The fingers moved slightly apart to ensure thumb and fingers can close fully and prevent friction when moving past each other.
- d) The front of the hand was gently sloped to grip objects better.
- e) The motors were reoriented to allow easier access to their cables and save space.
- f) Extra cut-outs were added for wiring to sit in.
- g) The rear was extended so the circuit board and relay could be placed within the main section of the hand, allowing a lowering of the height of the cover.





- h) Five side holes were added to place the LED battery level indicators and a switch. One large hole was added at the back so that the device could be charged without taking off the cover. To maintain the waterproofing rating, a block of flexible TPU was printed that could be pushed in as an interference fit to fill the hole when not in use.
- i) The mid-plate was added between the cover and the base plate of the hand to guide wires and constrain lateral movement of the electronics within the hand.

#### 3.4.4 JOINTS AND FIXTURES

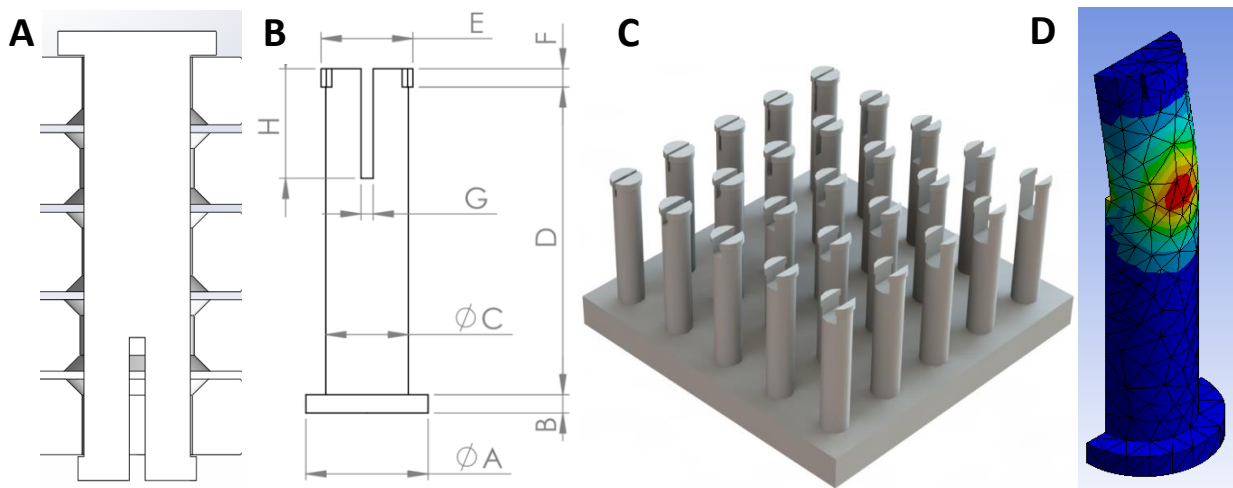


Figure 12: (A) Pin Locking System. (B) Dimensioning. (C) Pin Testing Rig. (D) FEA of Loading on pin.

The joints connecting the fingers to the palm ('knuckle' pins) and connecting the palm to the socket ('wrist' pins) were designed as simple push pins with lips which lock into place, shown in Figure 12(A). These pins, made from PETG, must be able to support the device when under its maximum load of 50 N (specified in the PDS) and the complex shape of the pins makes analytical calculations difficult and potentially inaccurate. For this reason, a testing rig, shown in Figure 12(C), was developed to enable testing of many different pin geometries – resulting in the optimal dimensions for both the wrist and knuckle pins being found through testing. Once the best pin was found, the results were validated using a finite element analysis (FEA) study, shown in Figure 12(D). This demonstrated the location of the weak point in the structure and provided values of the stress at this point when under loading – giving results of 27.8 MPa for the wrist pins and 32.9 MPa for the knuckle pins under a 50 N load. This corresponds to safety factors of 17 and 14.6 respectively, ensuring that the pins were more than strong enough to handle the maximum loading case set out in the PDS. The final dimensions of the pins are shown in Table 6, referencing the dimensions labelled in Figure 12(B).





Table 6: Pin Dimensions

Pin type	Dimension (mm)							
	A	B	C	D	E	F	G	H
Wrist Pin	10	1.5	6.75	25	7.5	1.5	1	9
Knuckle Pin	7.5	1	3.75	19.5	4.25	1	0.75	7.5

### 3.4.5 SOCKET DESIGN

As previously mentioned, this project focusses on the hand itself so suspension from the amputee is not a key part of this project. Socket design is a complex and advanced area of prosthetic design in its own right, so, a simple approach was taken – designing a basic socket that could be used with a demonstration stand or with an amputee for testing purposes. The design can be seen below in Figure 13, consisting of 3-D printed PLA. Although it is printed flat, the part is designed to be thermoformed around the amputee's stump by submerging it in in hot water above 52.6 °C (the glass transition temperature for PLA). By wearing an insulating neoprene sleeve, the amputee can safely form the socket around their stump and get a comfortable, snug fit.

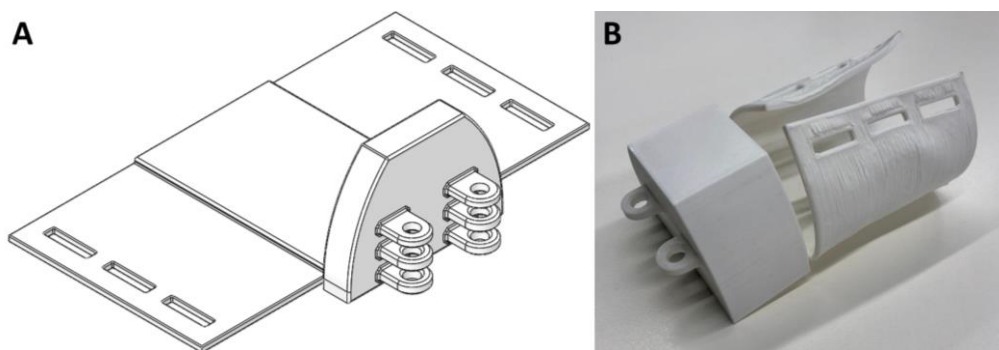


Figure 13: (A) Socket as printed. (B) Photograph of early stage prototype after thermoforming around a demonstration stand.

### 3.4.6 SENSOR STRAP AND CLIPS

Another minor, yet not to be overlooked part of this project was designing a comfortable armband which the user wears whilst controlling the prosthesis. The armband had to be able to securely hold the sensors over the correct muscles and allow adjustment for use by different individuals or for use on different parts of the arm. The design opted for was a 20 mm wide strap, secured in place with a



hook and loop ('Velcro') mechanism. The sensors sit in small plastic clips which can slide along the strap; the minimum diameter of the strap was 50 mm and the maximum diameter was 120 mm, enabling a wide variety of people to use it comfortably. The strap was made from elasticated fabric to enable it to change diameter slightly while in use – this is important to avoid the strap 'pinching' into the user's muscles as they contract, increasing the diameter of the arm. The assembly of the strap, clip and sensors is shown in Figure 14 (note: only one sensor is shown in this image, whereas the strap would typically house two).



*Figure 14: Sensor strap with a single sensor in place*

---

### 3.4.7 MECHANICALLY FUNCTIONING PROTOTYPE

The first functional prototype was made to test the combination of hard and soft materials in the finger and to look at the overall positioning of the fingers. A render of the prototype and the actual print can be seen below in Figure 15. During this test, the motors were simply turned on and off to test the functionality of the mechanical design.

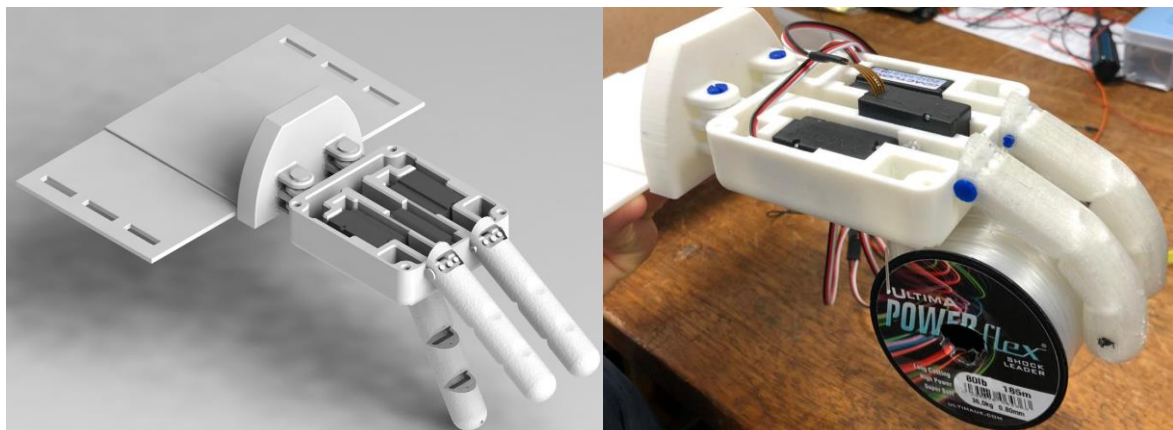


*Figure 15: A render of the working prototype, and it successfully picking up an example object*

The hand was successful in holding objects and hence demonstrated the functionality of the combination of materials. However, it struggled to grip flat surfaces (as opposed to wrapping around



objects) and could not fully close. This was due to the positioning of fingers - the two fingers were too close to each other which meant the thumb could not close at the same time as the fingers. Therefore, the two fingers were moved slightly further apart for the final design (as mentioned in section 3.4.3 **Error! Reference source not found.**).

### 3.5 CONTROL DESIGN

The fundamental principle of operation of this device is that two sensors can be housed in a strap over an antagonistic muscle pair. Specific movement patterns will cause one or both muscles to contract, which can be detected by the sensors and converted into a grip pose, as illustrated in Figure 16.

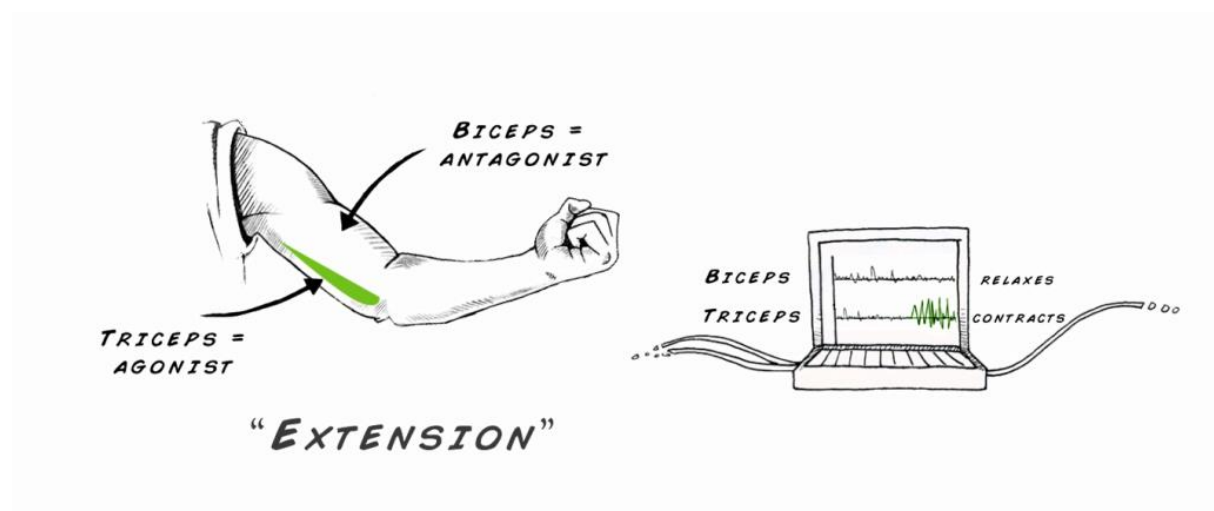


Figure 16: Basic principles of muscle sensing. Image adapted from (29).

Although this is simple in principle, developing custom software to acquire, process and classify signals in real time was one of the significant challenges of this project. Successful software should be able to do this with high accuracy, low latency and not be sensitive to 'noise' or non-target muscle movements. This section details the design of the control systems and software for the final prosthesis, with the reasoning and technical detail justifying it.

#### 3.5.1 PRELIMINARY TESTS

The first stage in developing the software for the device was to understand the signals being acquired from the MMG sensors. During this stage of discovery, a single MMG sensor was used in conjunction with an Arduino UNO board for data acquisition; the signals were then sent through a serial connection to a Python script where the data could be visualised.



The first test is shown in Figure 17, where the sensor was placed over the brachioradialis muscle of the test subject and the muscle was activated in four different ways throughout the test. The voltage output from the sensor was plotted against time for each muscle contraction to make the graphs. The top-left graph shows the results when no voluntary muscle contraction is performed; from this data, we can see that there is a messy high frequency noise in the data, as well as a significant 1 Hz noise (which we believe to be the microphone picking up the subject's heartbeat). The other three graphs show more muscle movement types: a three second isometric hold, a fast concentric then eccentric movement and a slow concentric then eccentric contraction. These graphs all seem to show a similar pattern – a high frequency, high amplitude set of spikes during the muscle contraction, immediately followed by a low frequency signal (which seems to represent the muscle returning to a relaxed state). We want the device to be able to recognise all these contractions as a user input, so the algorithm should be designed to recognise the low-frequency spike.

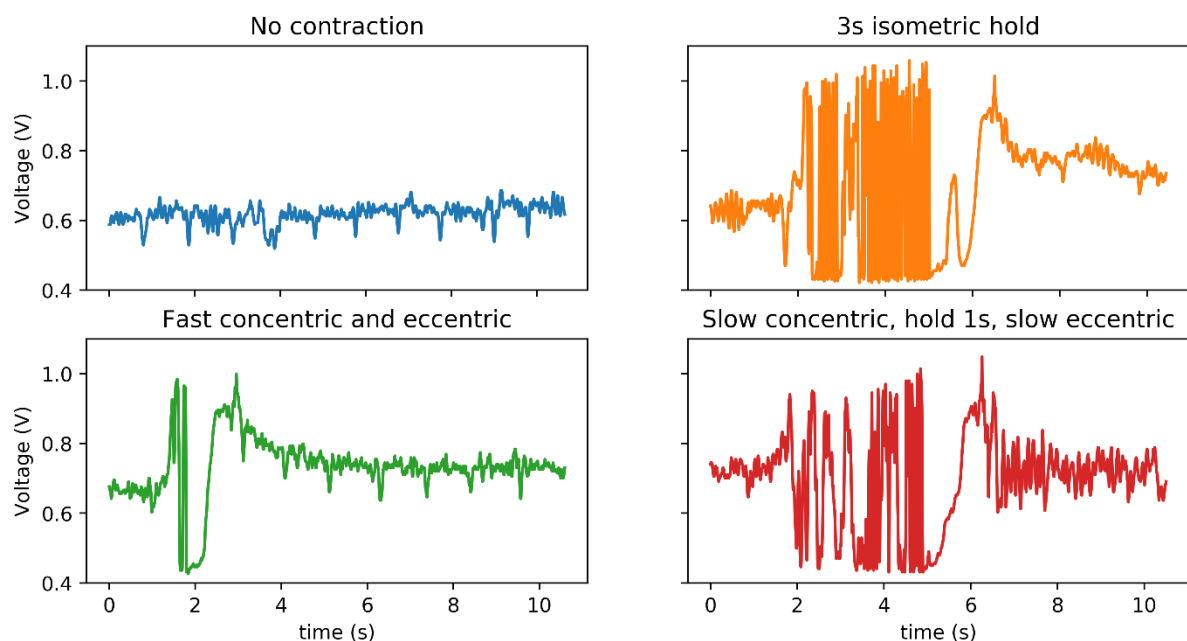


Figure 17: Raw data acquired from MMG sensors

The next tests were concerned with the optimal placement of the sensors, as well as their sensitivity to non-target movements. Since both the sensors are housed in a single armband over a muscle pair, there were three candidate locations for the positioning:

- ✦ Forearm (over the flexor digitorum and extensor digitorum pair)
- ✦ Below elbow (over the brachioradialis and extensor carpi ulnaris pair)
- ✦ Above elbow (over the biceps brachii and triceps brachii pair)



Figure 18 shows the results of these tests for the forearm strap placement. The two graphs on the left show the response from their respective muscles during the target movement (wrist extension and flexion). The two graphs on the right-hand side show the response of these muscles for a non-target movement (in this case, wrist pronation and supination were chosen).

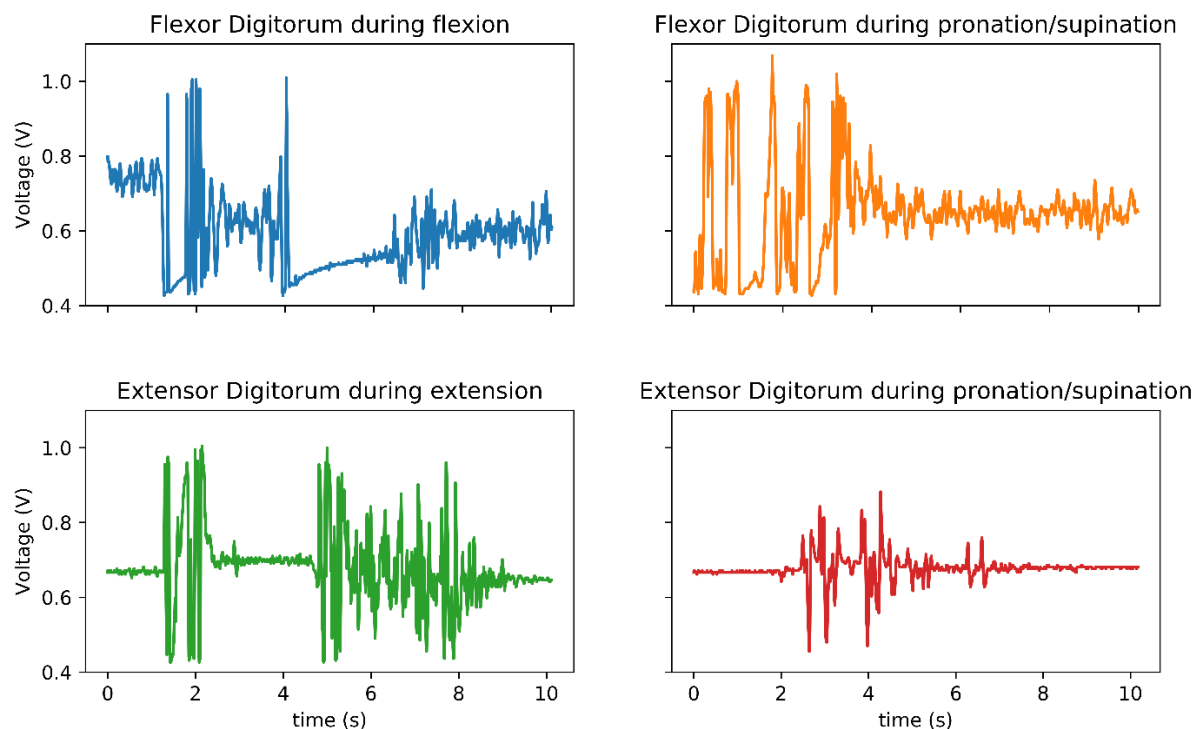


*Figure 18: Signals recorded from forearm sensor locations during target and non-target movements*

From this data, it is clear that these sensors are very susceptible to noise in the data – meaning that non-target muscle movements are almost indistinguishable from the target movement in many cases. This problem was found to be pervasive over all three of the sensor locations, so no location was deemed to be clearly superior and sensor placement can be decided by the preferences of the end user.

This problem of noise in the data means that, in order to avoid unintentional device actuation ('false positives'), the signal classification algorithm was designed to only recognise muscle contractions which occurred for longer than a certain period of time. It is unlikely that a non-target muscle movement would be sustained for a long period, so this enables the device to classify signals into intentional and non-intentional.



### 3.5.2 SIGNAL PROCESSING ALGORITHM DESIGN

Once the preliminary tests had been performed, the algorithm for processing and classifying the signals was designed. The first task was to filter the data – this is important because (as discovered in the preliminary tests 3.5.1) the important part of the signal is a low frequency spike which occurs during muscle activation. The final filter design was chosen by consulting the existing literature and selecting the same setup used in (23) – a fourth order Butterworth band-pass filter (5-100 Hz), with a sampling frequency of 1 kHz.

Once the signal is filtered, it must then be rectified and smoothed. The approach used in this project was to take the root mean square over a moving window of data – this is a common strategy used in EMG signal processing to output a result proportional to the power of the signal in the desired frequency range (30). The size of the moving window (N) was selected to be 500 samples (corresponding to 0.5 seconds of data at 1 kHz). This was chosen as a trade-off between signal to noise ratio (which scales with approximately  $\sqrt{N}$  (31)) and minimum length of muscle contraction required to activate the device (too long and it becomes cumbersome and tiring to use). Figure 19 shows the raw signal, filtered signal and RMS smoothed signal for a 3 second isometric muscle contraction (the y-axis units of these graphs are the output from the analogue to digital converter in arbitrary units).

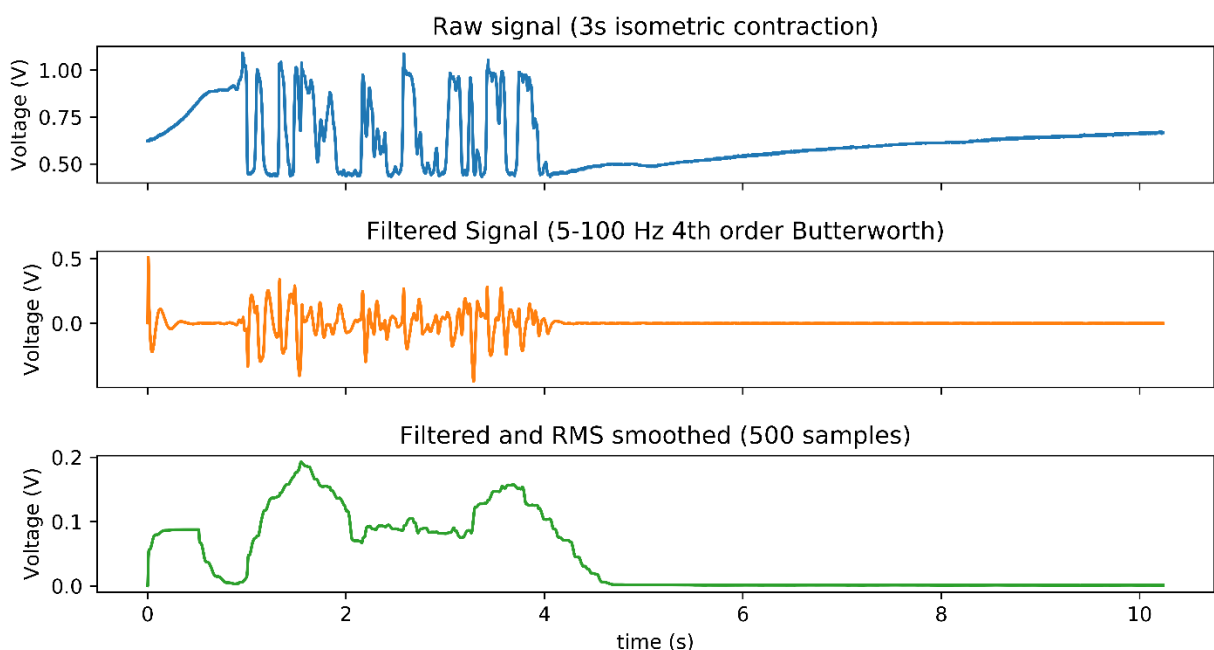


Figure 19: Signal processing of a 3 second isometric muscle contraction



The signals shown in Figure 19 demonstrate the effectiveness of this signal processing algorithm, converting a messy raw muscle signal into a simple, smoothed output which is proportional to the instantaneous power of the muscle contraction.

To classify this smoothed output signal, a simple digital implementation of a Schmitt trigger was chosen. This is where the muscle is registered as contracted once the smoothed signal rises above an upper threshold value and the muscle is then registered as relaxed once the signal falls below a lower threshold value. The separation of upper and lower threshold values prevents the registered muscle status from oscillating between contracted and relaxed due to noise in the data. For example, Figure 20 demonstrates the difference between a Schmitt trigger and simple comparator, using the same muscle data as Figure 19. Clearly, the Schmitt trigger correctly identifies the three second muscle contraction, whereas the comparator wrongly outputs two short contractions.

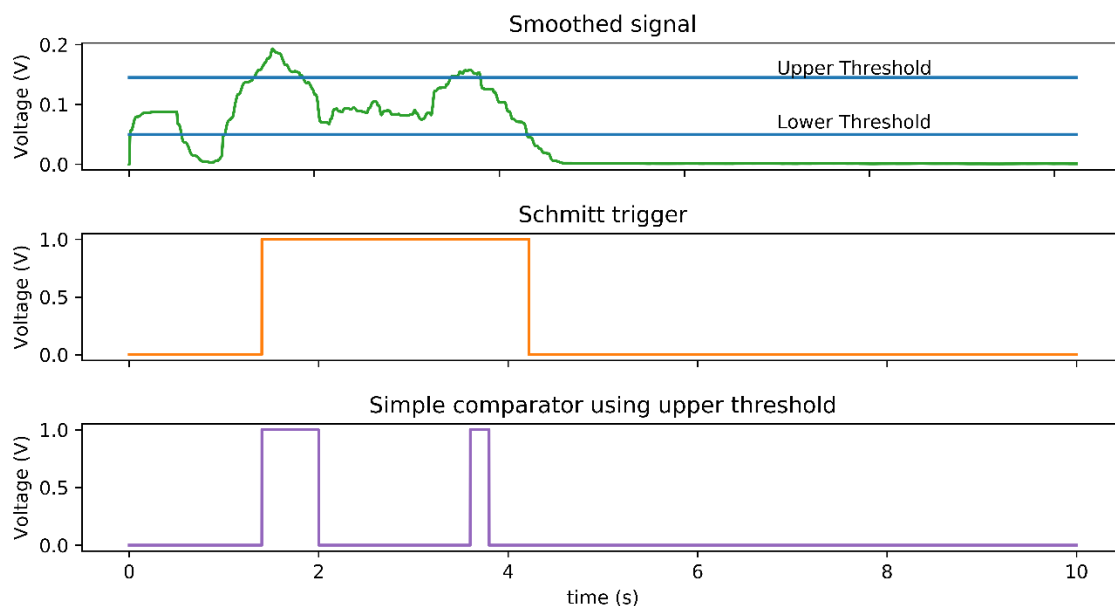


Figure 20: Comparison of Schmitt trigger against comparator for signal classification

Finally, once the incoming signals from both sensors have been classified to determine whether each muscle is contracted or not, the prosthesis can decide whether to change grip pose or not. The details of this are described in sections 3.5.3.1 and 3.5.4.2, where the device operating protocol and its implementation are discussed respectively.

### 3.5.3 OPERATING PROTOCOL AND USER EXPERIENCE

This section discusses the operating protocol of the device and user interface features. The three areas of consideration were: controlling the device in different grip positions, tuning the threshold value to individual preferences and battery management.





---

### 3.5.3.1 MOVING BETWEEN GRIP POSES

The three grip poses of the device are 'grip', 'point' and 'open' and it is important that moving the prosthesis between these poses is intuitive and easy to learn. The operating protocol involves the 'point' and 'grip' poses each being associated with one of the muscle sensors. The user can select one of these grips by simply contracting the relevant muscle and the open pose can be returned to by contracting that same muscle again. The state transition diagram depicting this protocol is shown in Figure 21 – in this example, the grip pose is associated with the biceps brachii and the point pose is associated with the triceps brachii.

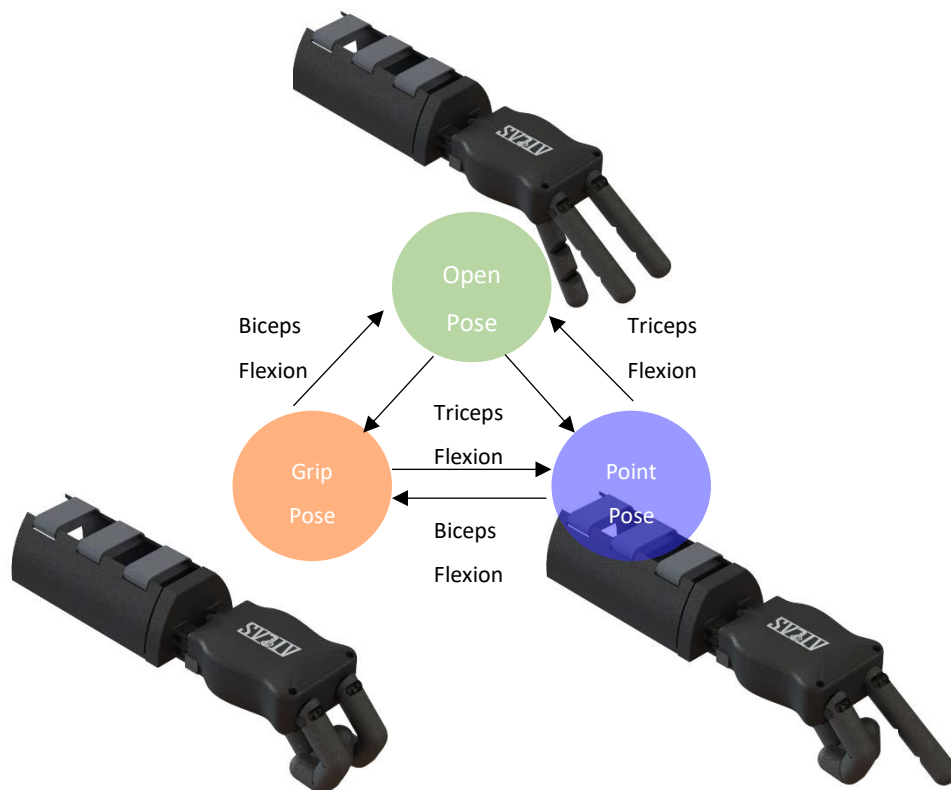


*Figure 21: State transition diagram for device poses, showing the working prototype performing each pose*

---

### 3.5.3.2 TUNING THRESHOLD VALUE FOR INDIVIDUALS

Since this prosthesis must be able to be used by different individuals, the signal classification algorithm must be able to be slightly changed to suit each user's physiology and preferences. For this reason, the upper threshold value for the Schmitt trigger can be altered using a potentiometer inside the device. When first setting up the prosthesis, each user should start with the potentiometer turned fully clockwise (representing the highest possible threshold value), then, perform one of the muscle movements associated with a grip pose (for example biceps flexion) whilst turning the potentiometer counter-clockwise. Once the device actuates, the user can stop turning the





potentiometer and re-attach the cover – the threshold value has now been customised to the individual. This process was designed to be straightforward and can be performed with one hand by an amputee – it also only needs to be performed once (when setting up the product for a new user).

---

### 3.5.3.3 BATTERY INDICATOR, CHARGING AND SLEEP MODE

Managing battery levels has the potential to be a stressful task for a user who relies on the prosthesis for daily life. To minimise this, four LEDs and a button are included on the side of the device (shown in Figure 22). A short press of the button causes the LEDs to light up to display the device battery level and a long press of the button puts the device into a power saving sleep mode. While in this mode, a relay inside the device disconnects the motor circuit from the battery and controller – making it safe to charge using the micro USB port on the side. The prosthetic hand was designed for people with a transradial amputation on their right arm, so the button and LED indicators are on the left side of the device for ergonomics.



*Figure 22: Rendering of LED and button user interface*

---

### 3.5.4 SOFTWARE IMPLEMENTATION

The software was implemented in C and a modified version of the Arduino library (32) was used to provide meaningful names to the pins on the microcontroller and to allow higher level, readable code without having to focus on the specific architecture and registers of the microcontroller used.

One challenge of this project was implementing the control and UI algorithms to run on a microcontroller in real time and with low latency; for this to be the case, the main loop of the program must run faster than the sampling frequency (1kHz). Achieving this involved implementing the software to be efficient in terms of both space and time – some of the main measures taken when implementing the code are described here and ‘big O’ notation is used to describe how these algorithms scale.



---

#### 3.5.4.1 SIGNAL PROCESSING (MOVING WINDOW RMS CALCULATION)

The moving window involves each sensor having a 500-sample integer array associated with it. These arrays are the most memory-intensive part of the software and, unfortunately, there is nothing that can be done about the space requirements as they scale linearly with the size of the arrays,  $O(N)$ . However, it is extremely important to ensure that the process of adding and ejecting data from the queue is as efficient as possible – as well as the calculation of the root mean square. A snippet of the implementation for these processes is shown in Figure 23.

```
1 // Replace the oldest value in the array with the new data,  
2 // but temporarily store it in the oldData short  
3 short oldData = movingWindow[position % LENGTH]  
4 movingWindow[position % LENGTH] = newData;  
5  
6 // Find the RMS of the window  
7 sumSquares -= oldData * oldData;  
8 sumSquares += newData * newData;  
9 int RMS = sqrt(sumSquares / LENGTH);  
10  
11 position ++; // increment position in array
```

Figure 23: Efficient implementation of moving window RMS smoothing

This code involves storing the current position in the array and the current sum of the squares of the array and simply using the modulo operator to make the array circular. Each time new data comes out of the filter, the oldest value is looked up in the array, stored in a temporary variable and replaced by the newest value. The new root mean square value is then calculated by simply subtracting the square of the old value from the sum of the squares running total and adding the square of the new data to it. The running total is then divided by the size of the moving window and square rooted to find the RMS value of the window. This code is particularly efficient because it scales with  $O(1)$ , meaning that the computational time is constant no matter the size of the moving window. This helps the program run in real time, where the program must loop faster than the sampling rate of 1 kHz.

---

#### 3.5.4.2 SIGNAL CLASSIFICATION

When implementing the signal classification algorithm, computational speed was unlikely to be an issue because the input data (the processed signal from each muscle) is simply a pair of integers, so the algorithm does not need to be designed with scale in mind. The most important factor in the design of this section was code readability and maintainability; for this goal, a state transition table was the natural choice to use. This is simply an array which takes three inputs: the current pose of



the device and the status of the two muscle sensors (either detecting muscle contraction or not). To classify the muscle signals into a target grip pose, the device simply uses the table to look up which pose should be activated (shown in Figure 24). The advantage of this method is that the programmer can easily change the operating protocol by simply changing the numbers in the table – this enables software updates to be effortlessly and rapidly developed if needed.

```

38 // Takes the status of both muscles and classifies it into a pose
39 int classifySignal(int currentPose, int bicepState, int tricepState)
40 {
41     // The first index is for the current pose
42     // The second index is for the bicepState
43     // The third index is for the tricepState
44     int stateTable[3][2][2];
45
46     // current pose is open
47     stateTable[0][0][0] = 0; // no change, so stay open
48     stateTable[0][0][1] = 2; // tricep, so point
49     stateTable[0][1][0] = 1; // bicep, so grip
50     stateTable[0][1][1] = 0; // both active, so dont change
51
52     // current pose is grip
53     stateTable[1][0][0] = 1; // no change, so stay grip
54     stateTable[1][0][1] = 2; // tricep, so point
55     stateTable[1][1][0] = 0; // bicep, so return to open
56     stateTable[1][1][1] = 1; // both active, so dont change
57
58     // current pose is point
59     stateTable[2][0][0] = 2; // no change, so stay grip
60     stateTable[2][0][1] = 0; // tricep, so return to open
61     stateTable[2][1][0] = 1; // bicep, so grip
62     stateTable[2][1][1] = 2; // both active, so dont change
63
64     return stateTable[currentPose][bicepState][tricepState];
65 }

```

Figure 24: State transition table for signal classification

## 3.6 ELECTRONIC DESIGN

To ensure that the product control and power requirements could be met, a key consideration was the selection of physical electronic components and the designing of a circuit that can allow the full functionality envisaged in a compact form factor. This section describes the physical electronic design for the final product and the reasoning behind the design decisions.

### 3.6.1 MECHANOMYOGRAPHIC SENSORS

Due to the nature of MMG muscle signals as low-frequency vibrations, many commercial microphones are capable of picking up these signals. Fortunately, however, *SERG technologies* (a spin-off company from Imperial's Biomechatronics laboratory) kindly gave us three sensors they had developed for commercial use. These sensors consist of a Knowles SPU1410LR5H-QB MEMS microphone, housed in a 3-D printed casing – shown in Figure 25. The shape of the casing directly affects the quality of the signals acquired and the optimal shape was found by Posatskiy and Chau



(33). These sensors were more than suitable for this project, so development of our own sensing unit was not necessary.

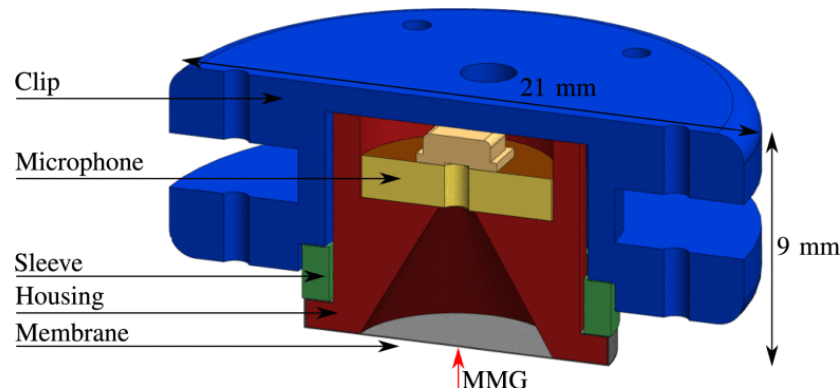


Figure 25: MMG sensing unit configuration, adapted from figure 1 of (34).

---

### 3.6.2 CONTROLLER

Selecting an appropriate microcontroller was the centrepiece of the electronic circuit design, with several requirements such as memory, clock speed and input / output (I/O) factoring into the final choice. Another consideration was whether to purchase a standalone controller and develop our own printed circuit board (PCB) to fit the electronics or to purchase a general-purpose development board, such as those made popular by Arduino in recent years. It was decided early on in the project that the latter approach would be more suitable because the design and manufacture of a suitable PCB would be a significant drain on the project's time and resources, with comparatively few benefits compared to using an 'off-the-shelf' solution.

When selecting the microcontroller, it was vital to select one with sufficient memory and clock speed to run the taxing signal processing code in real time. Early testing made use of an Arduino UNO board, which contains an 8-bit controller with 32 kB of flash memory and a 16 MHz clock speed, however, it quickly became apparent that this board lacked the required memory and speed to run the code when two sensors were used. After careful consideration, the Adafruit feather M0 Basic board was selected – this contains a 32-bit microcontroller with 256 kB of flash memory and a clock speed of 48 MHz, providing several benefits over the less powerful Arduino. The Adafruit board is fast enough to process the data from both sensors in real time and also has enough memory to easily hold the 500-sample moving window (described in section 3.5.2) in working memory, where the Arduino could only hold a maximum of 100-samples. Other advantages of this board are the inbuilt battery management and charging systems as well as a low-power sleep mode; this enabled user experience features such as a standby mode and an easily accessible micro USB charging port to be easily integrated into the product.



---

### 3.6.3 MOTORS

The final concept, developed following the morphological analysis outlined in section 3.3.3, identified linear motors as the primary actuation method. Maximum force and power requirements were the main factors considered when choosing motors as they must be capable of meeting the grip strength requirement set out in the PDS, whilst not demanding a large battery. Stroke length was also important because the motors must be able to pull the fingers through their full range of motion, without being bulky or heavy. These strict requirements limited the scope of selection significantly, with the Actuonix PQ-12 linear servo motors standing out as the natural choice for this project. Each PQ-12 can provide a maximum force of 50 N, consumes approximately 3 W when stalled and has a stroke length of 20 mm; these motors lie on the premium end of the spectrum (costing a minimum of £ 85 per motor), however, discussions with experts in the field such as Alex Lewis and our supervisor Dr Ravi Vaidyanathan justified this expense as they emphasised the importance of strong, reliable grasping in prosthetic hands. Figure 26 shows the motors in use in a functional prototype of the device.

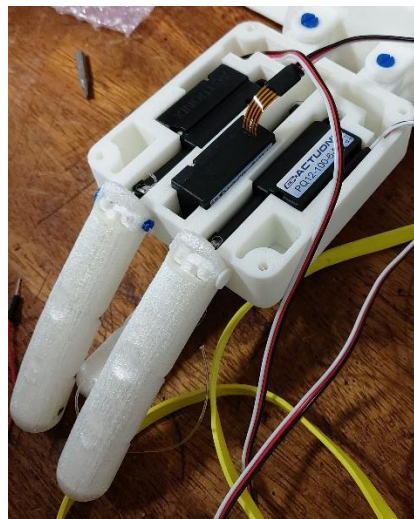


*Figure 26: Actuonix PQ12 motors displayed in working prototype*

---

### 3.6.4 POWER SUPPLY AND CHARGING

---

#### 3.6.4.1 BATTERY SELECTION

Battery selection involved balancing capacity, discharge current, voltage and size. These design parameters are each crucial and required careful calculation to ensure that the best battery was chosen. The most compact batteries available were 3.7 V LiPo batteries, which are ideal for powering the Adafruit 3.3 V board – one slight complication though is that the PQ-12 motors require a 6 V voltage source. This was easily solved by the inclusion of a ‘buck-boost’ DC-DC voltage



converter to step up the voltage which, naturally, increases the current draw of the motors by 74 %, due to conservation of energy ( $P = IV$ ) and inefficiencies in the converter. This high current draw meant that the battery had to be selected with a large enough capacity to operate with the battery life specified in the PDS and to withstand the maximum current draw of the motors under maximum load. The minimum necessary capacity was calculated using Equation 2, using the parameters listed in Table 7.

Table 7: Parameters used in battery calculations

Parameter	Physical Meaning	Value	Justification (where necessary)
$N_m$	Number of motors	3	
$i_m$	Current draw of one motor during an operation	0.25 A	Experimental evaluation of motor current using ammeter
$N_{ops}$	Number of operations per hour	60	Heavy use will average out to one operation per minute
$T_{life}$	Battery life	12 h	Minimum battery life specified in PDS
$\frac{V_{motor}}{V_{battery}}$	Current magnification caused by boost converter	1.622	Simply divide output voltage (6 V) by input (3.7 V)
$\eta_{boost}$	Efficiency of boost converter	0.93	Specified in converter datasheet
$i_c$	Current draw of microcontroller	0.05 A	Experimental evaluation of current draw using ammeter
$t_{op}$	Time taken per motor operation	$\frac{3}{3600}$ h	Each motor operation takes approximately 3 seconds

$$N_m i_m N_{ops} t_{op} T_{life} \frac{V_{motor}}{V_{battery}} \eta_{boost} + T_{life} i_c = \text{Minimum capacity (Ah)} \quad \text{Equation 2}$$

The minimum battery capacity required was calculated as 1.49 Ah. Due to the need for a reasonable safety factor on battery life, the battery chosen was a 3.7 V, 2Ah LiPo – capable of delivering 2 A under continuous discharge.



---

#### 3.6.4.2 ISOLATING RELAY

When the device is in sleep mode, it is important that the motors are electrically separated from the battery to prevent constant unnecessary current draw (and to prevent backflow whilst charging). It was decided to do this using a latching relay, which can be toggled by the microcontroller when the user pushes the power button. Fortunately, Adafruit produce an 'off-the-shelf' solution to this problem in the form of a latching relay board which simply stacks on top of the microcontroller board – the 'FeatherWing relay'. This provided a compact and elegant solution to the problem of isolating the motor circuit (depicted in Figure 27) and was superior to a mechanical switch because it does not add any complexity to the user interface or operating protocol.

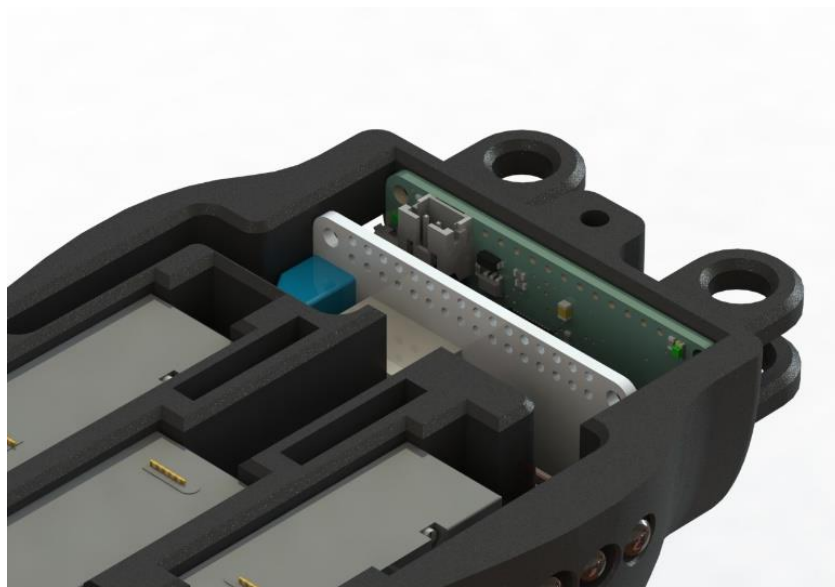


*Figure 27: Rendering of Adafruit feather microcontroller board and FeatherWing relay in the final product*

---

#### 3.6.5 OVERALL CIRCUIT

The full circuit diagram is shown below in Figure 28. This is a demonstrative simplified version rather than a full layout drawing. For example, the FeatherWing latching relay contains a number of inbuilt transistors and logic gates as drivers for the relay, but these are not shown on the below diagram for simplicity.





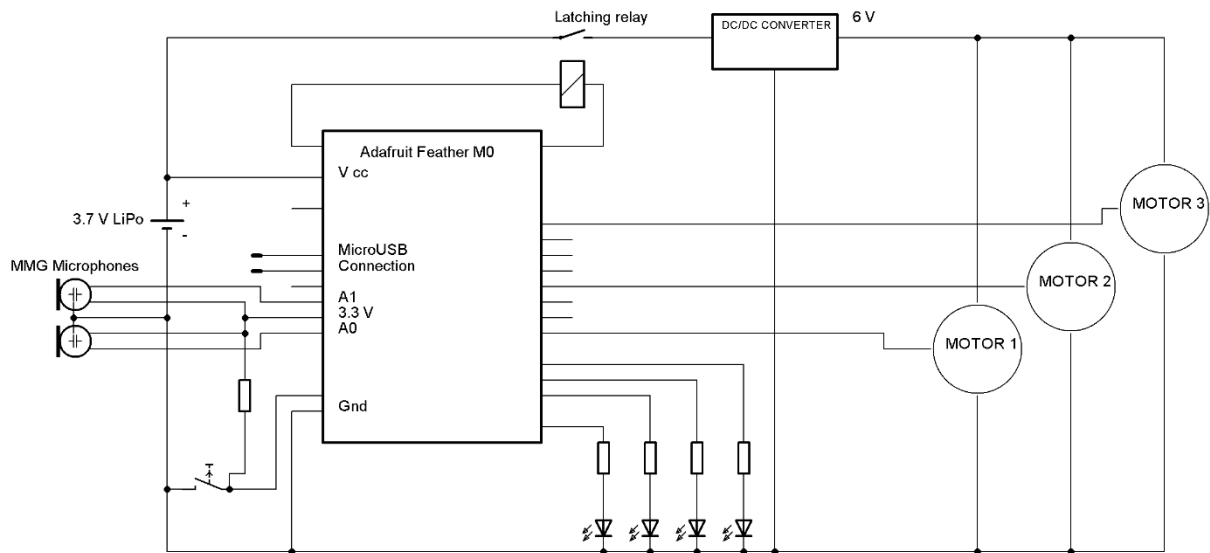


Figure 28: Demonstrative circuit diagram of electronic system

### 3.7 FINAL DESIGN

The figure below shows the final prototype produced, the ATLAS Arm, on a display stand and mounted to a plaster of Paris arm cast. The final prototype consists of TPU-PLA composite fingers, a smoothed hand section with feature integration such as LED battery level indicators and a button-operated sleep mode, the logo printed into the cover, a moulded wrist unit and an MMG sensor strap. The assembly and manufacture of the final prototype is detailed in section 4.

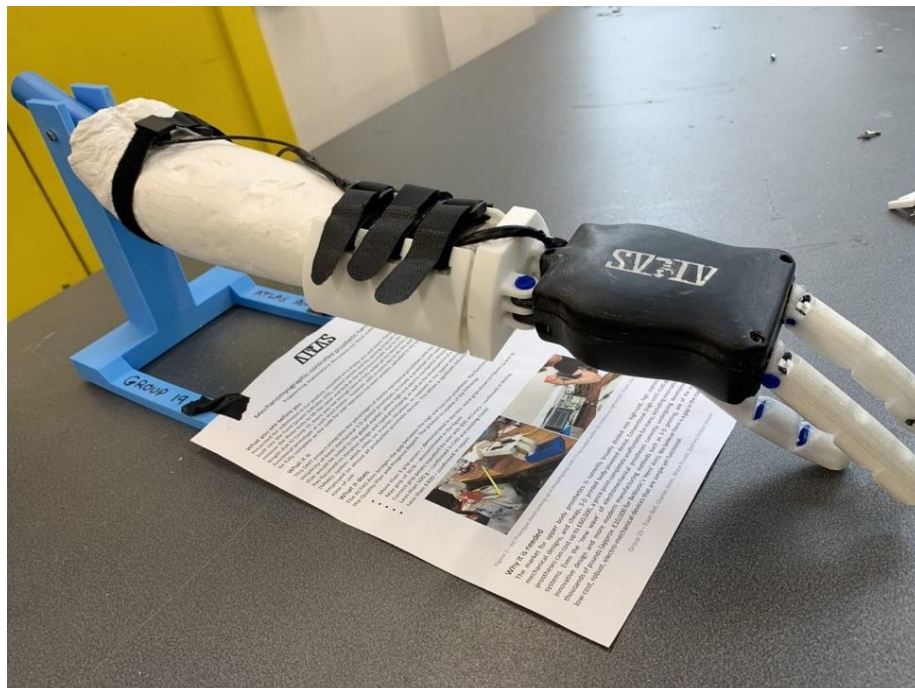


Figure 29: Final product on display





## 4 MANUFACTURE AND ASSEMBLY

Having discussed the overall design of the product, it is important to now look at the manufacturing and assembly. A large amount of this work was done in parallel with the design process, as our chosen manufacturing method of 3-D printing had a large impact on design. In this section we will cover the reasoning behind our choices of manufacturing method and material selection. We will also cover the assembly details for both the electronics and the mechanical hand.

### 4.1 METHODS AND JUSTIFICATION

Fundamental to the project from the beginning was the desire for the product to be manufactured in a decentralised fashion. This limited the range of manufacturing methods to those reasonably available to engineers and hobbyists who might volunteer to make the prosthesis for a local amputee. Although some methods (such as laser cutting) can be used to manufacture parts accurately for low cost, they are often relatively inaccessible, especially in developing countries – making them unsuitable for this project. Desktop 3-D printers are fast becoming the manufacturing method of choice for makers on a budget and, with an estimated 500 000 desktop printers sold in 2018 (35), 3-D printing stood out from the beginning as an important manufacturing method to utilise. In fact, an organisation, E-NABLE, already exists to connect amputees with local volunteers who can 3-D print open sourced body-powered prosthetic designs (36). Another advantage of 3-D printing is the speed and low-cost for small- batch production, typically considered best-in-class for polymers; repairs and replacements are also accelerated, with end users simply able to print replacement parts instead of sending the entire device into a central facility for repair.

There are many different types of 3-D printers, with the most prevalent being fused deposition modelling (FDM) printers, however, all 3-D printers follow the same basic principle. First a CAD file is put into a slicer software which takes the model, cuts it into layers and writes code which is inputted into the printer. The printer then constructs the model layer by layer. In FDM printers the layers are printed by extruding a “string” of plastic, as shown in Figure 30.

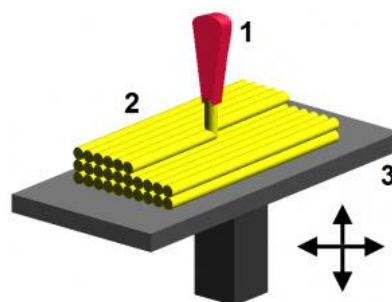


Figure 30: Fused deposition modelling. Image from 3DInsider (37).



All parts manufactured in this project were produced on one of the group's two Creality Ender 3 machines; this is one of the most popular commercial 3-D printers available and can be purchased for the entry level price of £ 150, making it a reasonable assumption that any hobbyists making our product will have a machine of similar quality. One feature this printer boasts is a heated print bed. This feature is extremely useful in preventing warping, which occurs when the temperature gradient across the part is too large and results in sections contracting at different rates, deforming the printed part. It is therefore advantageous to have a heated bed as it will result in more accurate parts. Although this feature is not present on all printers, most modern printers (such as the Ender 3) generally have this as standard.

## 4.2 MECHANICAL CHARACTERISTICS OF FDM PRINTED PARTS

There are inherent structural and mechanical issues with FDM parts, which can often dissuade engineers from selecting this as a primary manufacturing process. Some of these problems include:

- ⚡ The extruded filament bonding poorly to the already partially cooled polymer layer below (poor layer adhesion).
- ⚡ Gaps occurring between extruded filaments.
- ⚡ Rough surface finish due to the layered nature of construction.
- ⚡ Anisotropic material properties, such as weakness in the direction perpendicular to layers.

These limitations can be mitigated through careful design of mechanical parts and experience in selecting optimum print settings. The following section (4.3, design for 3-D printing) explores many of the manufacturing-specific decisions made during this project, including tests which were performed to provide evidence for them. Testing (detailed in section 6) was also performed on prototype parts to ensure that these potentially negative characteristics did not affect the product's ability to perform according to the PDS.

## 4.3 DESIGN FOR 3-D PRINTING

Having selected FDM 3-D printing as the primary manufacturing method for this project, it was crucial to ensure that all parts were designed with this manufacturing method in mind. This section summarises the design decisions and iteration that occurred as part of this design for manufacture philosophy.

---

### 4.3.1 PRINT ORIENTATION



It is a well-known fact that 3-D printed components are anisotropic in that they have different material properties depending on the orientation the part is loaded in. Therefore, an experiment was done to assess the strength of printing in the different orientations with the materials selected.

---

#### 4.3.1.1 TESTING METHOD

In this experiment, six specimens with dimensions 5 x 20 x 60 mm were printed in both PET-G and PLA (two printed in each orientation). The specimens were then clamped in an Instron tension and compression machine with a 24.75 mm gap between the clamps. They were then pulled at a rate of 5 mm min<sup>-1</sup> and the displacement and load were recorded over time. The specimen was pulled until the load dropped by 60 %, which occurred after rapid brittle fracture. The load and displacement were then converted into stress and strains using Equation 3. Strain against stress graph were plotted, and the Young's Modulus was then given by the gradient of the linear section of the graph (before significant plastic deformation occurred). The moduli for each orientation were then averaged. The ultimate tensile stress (UTS) and the engineering stress that the specimen reached before fracture were also found.

$$\text{Stress} = \frac{\text{Force}}{\text{Cross Sectional Area}}, \text{ Strain} = \frac{\text{Displacement}}{\text{Exposed Length}} \quad \text{Equation 3}$$

---

#### 4.3.1.2 TESTING RESULTS

The results of the experiment are found below in Table 8. The data shows that although the difference in Young's Modulus is small, there is a larger difference in the ultimate tensile strength, with the strongest orientation being involving printing along the axis of the thin but long edge and the weakest being printing along the axis of the short thin edge. The reasoning behind this is complex. When pulling the specimen printed on the short thin face the layers are getting pulled apart, whereas in the other two orientations the fibres are in tension, rather than the bonds between the layers. This implies that interlayer adhesion is the key variable in the strength of the print. The difference between the other two orientations will therefore also be due to the inter layer adhesion. Since the layers printed along the thinner edge are printed quicker, they are warmer when the second layer is added, meaning interlayer adhesion is better, explaining the observed results.

Thus, it was found that it was most important to avoid printing in an orientation that would mean the load applied would be perpendicular to printing plane. With secondary importance, it would also be important to try and print in an orientation that would mean smaller layer area, so that each layer printed quicker and therefore the interlayer adhesion would be higher.



Table 8: Results of Print Orientation Experimentation

Material	Face on Build Plate	UTS (MPa)	+/-	E (GPa)	+/-
<b>PETG</b>	Fat Face (20x60mm)	20.851	3.103	0.455	0.022
	Thin Long Face (5x60mm)	35.576	2.027	0.529	0.044
	Thin Short Face (5x20mm)	10.696	4.647	0.496	0.064
<b>PLA</b>	Fat Face (20x60mm)	22.299	14.465	0.497	0.213
	Thin Long Face (5x60mm)	25.695	10.111	0.535	0.119
	Thin Short Face (5x20mm)	9.557	1.200	0.584	0.081

#### 4.3.2 SIZING AND TOLERANCES

A second issue that arises with 3-D printing is that tolerances cannot be applied to the printer as it is printing. The slicing software will take the 'perfect' CAD model and write code to make the printer print to the exact nominal dimensions of the model. The printer itself is not perfect and therefore the print will not have the exact dimensions of the model. This is compounded by factors such as shrinkage where, as the deposited polymer cools, the polymer becomes less amorphous and more crystalline – increasing the density and reducing the volume of that section of the part. Due to the low thermal conductivity of polymers, and relatively high print temperatures, shrinkage is aggravated in thicker parts as the centre of the part cools slower than it would near the surface, allowing greater time for chain re-alignment and resulting in higher crystallinity. These factors can cause problems when printing parts with tight tolerances, so two methods were used to mitigate against them.

Firstly, parts with important tolerances were printed with a variety of slightly differing nominal sizes, this allowed them to be tested experimentally to determine the quality and consistency of the fit. The second method involved, where possible, designing regions with tight tolerances to dissipate heat during printing – hence reducing the effect of shrinkage on that region of the print. This is demonstrated in Figure 31, which shows the connectors which attach the palm to the socket. The high surface area of these connectors was intentionally designed to allow them to act as thermal fins, dissipating heat and preventing warping which might affect the fit.





Figure 31: Rendering of palm connector points

#### 4.3.3 SUPPORTS

An area which majorly impacts print quality is support structure. This is something unique to 3-D printing due to the layer by layer construction and is necessary when the part contains large overhangs or bridges. Printers tend to struggle when printing on thin air for significant distances, causing the resultant structure to sag or the print to fail entirely. Support structure is therefore essential for these overhangs; however, minimising support structure is typically a good idea to reduce material consumption and limit the amount of necessary post-processing. To minimise the necessary supports, parts were printed in the orientation which leads to the fewest overhangs (provided the print orientation did not create structural weak points). Parts were also designed in such a way to minimise support structures, a skill we improved at considerably throughout the project. Figure 32 shows two iterations of the socket design, with support structure depicted in green. The second design (B) was made with the goal of reducing support material explicitly, after it was discovered that the support material on first design (A) was difficult to remove, leaving plastic sprues (residue) which worsened the finish. Design B required only 31 % as much support material as A, was faster to print and had a better surface finish.

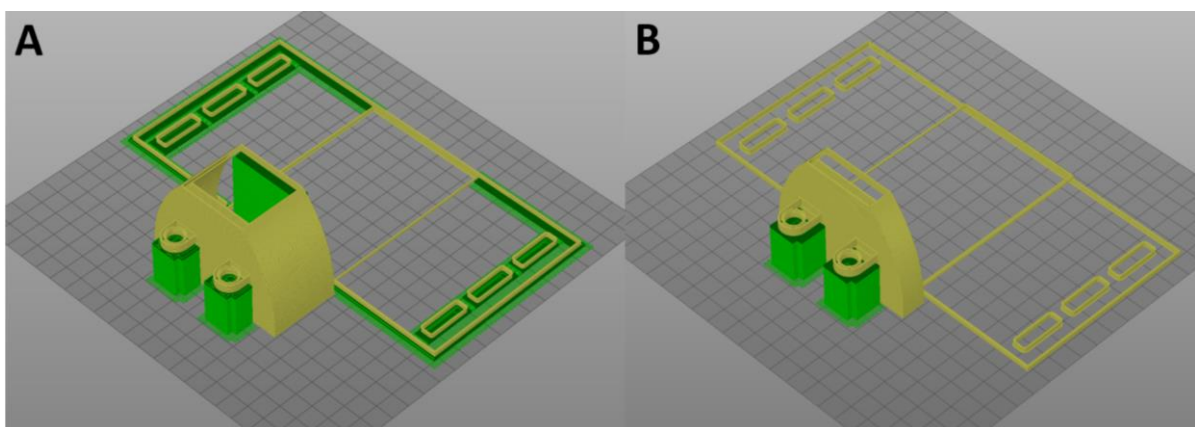


Figure 32: First iteration of socket design (A) and socket after being redesigned to minimise support material (B).



#### 4.4 PRINTING WITH PETG, PLA AND TPU

A common misconception is that changing material on an FDM printer is as simple as just changing the print temperatures. Due to the different properties of each material, there are many different settings that had to be tuned to ensure the prints were successful and did not suffer from mechanical problems. This involved lengthy research and experimentation, combined with experience to get the settings right.

PLA is the simplest material to print with, hence a reel of it is normally delivered with any new 3-D printer. The optimal print settings for this material are well known so this material required little work to produce good results.

PETG is a less commonly used material and although there is a large amount of information about printing with it, differences in PETG composition between manufacturers (combined with differences in commercial printers) made it difficult to initially produce ideal results. After several rounds of trial and error, we found that with PETG produced by eSUN, the filament printed best with nozzle temperature of 210 °C and build plate temperature of 100 °C.

TPU was the hardest material to print in due to its flexibility, as it would easily buckle while being fed into the nozzle and therefore result in under-extrusion. Another issue was that support structures were extremely difficult to remove due to the flexibility of the material. The final issue was that parts that were tall in the z-axis flexed and bent during printing, meaning filament was extruded onto the parts in the wrong place. These issues were corrected by lowering the print speed significantly, orienting parts so they have a large build base and increasing the gap between support structures and the actual part. PVA glue was also applied to the build plate to improve first layer adhesion.

A summary of the key printer settings can be seen below in Table 9.

*Table 9: Printer Settings for the different materials*

	PLA	PETG	TPU
<b>Print Speed (mm/s)</b>	30	30	8
<b>Print Temperature (°C)</b>	180	210	200
<b>Bed Temperature (°C)</b>	60	100	30
<b>Extra Adhesive on Plate?</b>	None	None	PVA glue



## 4.5 ASSEMBLY OF ELECTRONICS

Assembly of the electronics in the final product was designed to be simple, with electronic components being wired together outside of the casing and simply lowered into place. The wires would be soldered into place and heat shrink sleeves would be wrapped over any exposed wire to provide electrical isolation for user safety and to remove the possibility of any short circuits.

Unfortunately, due to the college shutdown, assembly of electronic components in the final product was unable to be completed (a topic further discussed in section 7.1, the effect of college shutdown on this project); although we estimate that an individual with soldering experience would be able to complete this process in under two hours. Figure 33 shows the positioning of the electronics in the final product.

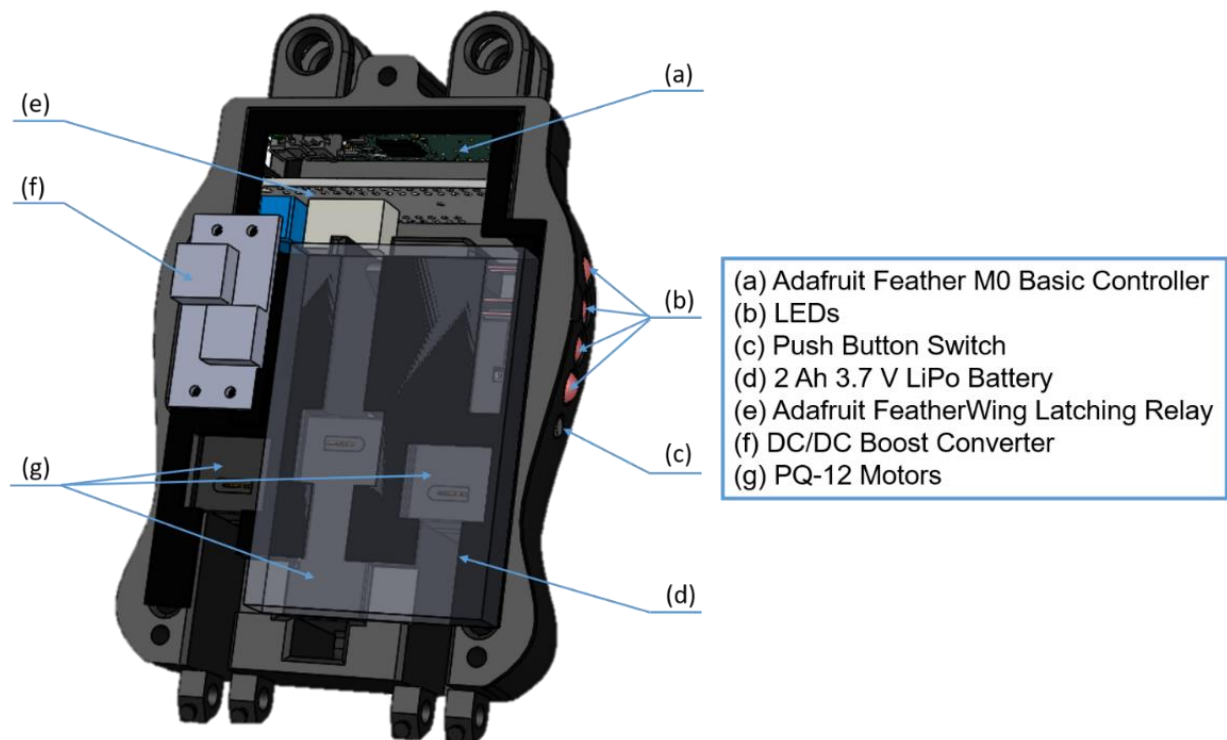


Figure 33: Electronics Layout

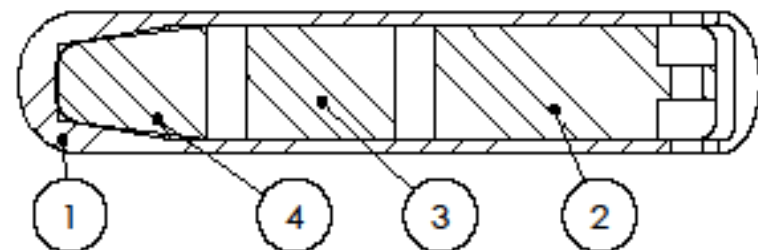
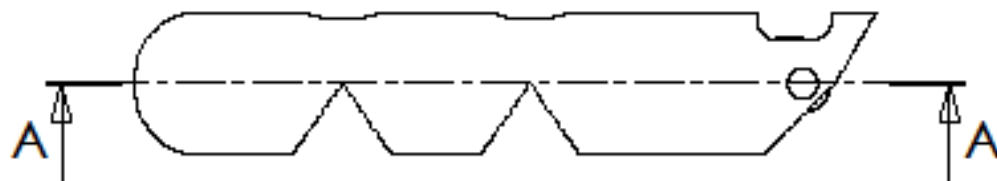
## 4.6 OVERALL ASSEMBLY

The overall assembly of the prosthesis, shown in the assembly drawing on the following page, is a four stage process: first assemble the electronics as in Figure 33; then assemble the three finger subassemblies; attach the finger subassemblies to the palm, threading the fishing wires through to the motors; and finally attach the socket to the palm. Once that has been complete, simply screw the cover onto the palm with three M3 bolts and the product is fully assembled.





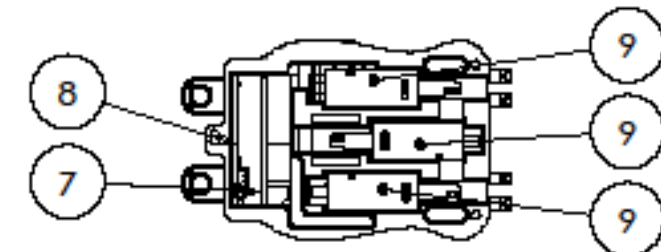
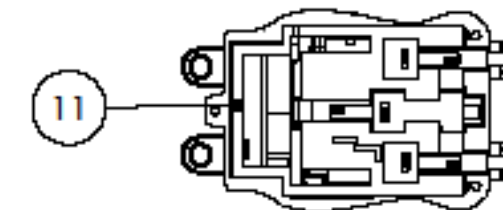
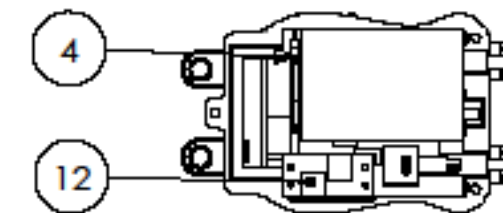
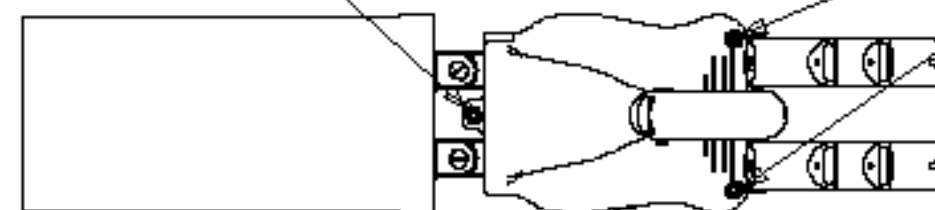
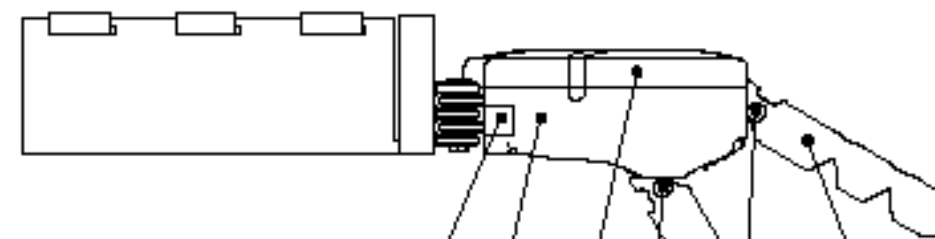
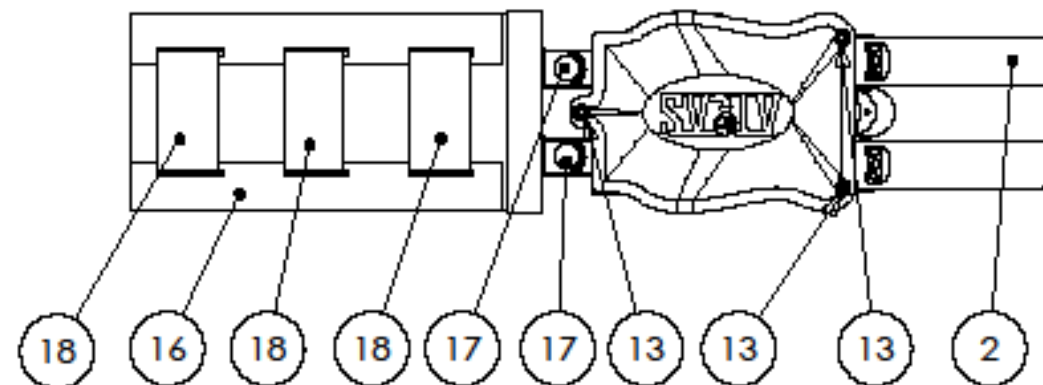
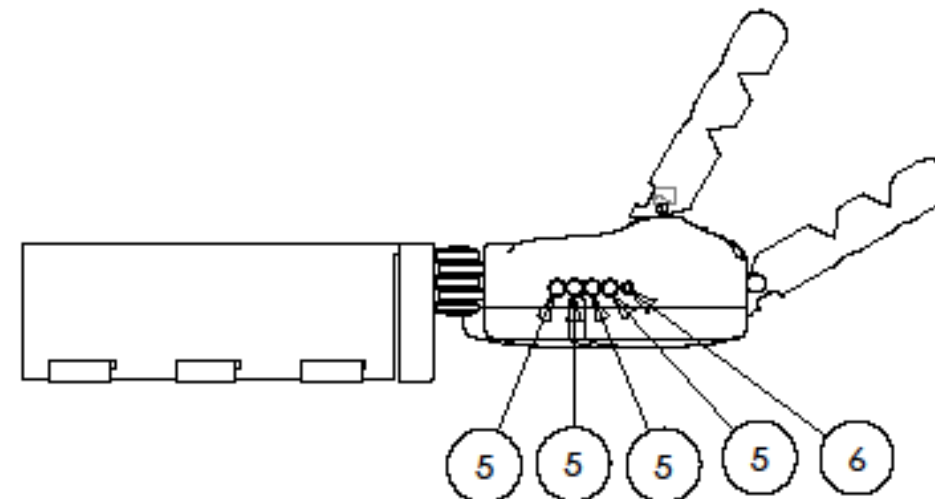
# FINGER ASSEMBLY SCALE 1:1




## SECTION A-A SCALE 1:1

ITEM NO.	PART NUMBER	QTY.
1	OUTER FINGER	1
2	PHALANGE 1	1
3	PHALANGE 2	1
4	PHALANGE 3	1

ITEM NO.	PART	QTY.
1	MAIN HAND	1
2	FINGER ASSEMBLY	3
3	HAND COVER	1
4	RS PRO 3.7V, LITHIUM POLYMER BATTERY 2AH	1
5	LED	4
6	BUTTON SWITCH	1
7	FEATHERWING LATCHING MINI RELAY BOARD	1
8	ADAFRUIT FEATHER CORTEX-M0 PROTO BOARD	1
9	PQ12 MOTOR	3
10	KNUCKLE PIN	3
11	MID PLATE	1
12	DC/DC BOOST CONVERTER	1
13	M3 X 16MM SOCKETHEAD BOLT	3
14	M3 NUT	3
15	CHARGING PORT COVER	1
16	SOCKET SECTION	1
17	WRIST PIN	2
18	FABRIC SECURING STRAPS	3



HAND WITHOUT LID TO SHOW  
THE LOCATION OF  
ELECTRONICS

TOLERANCES		THIRD ANGLE PROJECTION		MATERIAL:		TITLE:		Imperial College London Department of Mechanical Engineering	
X	±0.5			ALL DIMENSIONS ARE IN MILLIMETRES		ATLAS ARM			
X.X	±0.1								
X.XX	±0.02								
SURFACE FINISH MACHINED FACES Ra 6.3									
NAME		DATE		DO NOT SCALE DRAWING		DWG No.		SHEET 1 OF 1	
DRAWN		B.PUSZET		10/03/20		GRP19 - ATLAS ARM - 01			
CHECKED		C.JONES		11/03/20					
APPROVED		T.SEDDON-DEANE		12/03/20		A3		SCALE 1:3	



## 5 PRODUCT COST AND BUDGET

This section briefly assesses the budget of the project and the cost of the final product. It was of upmost importance during the project to not run over budget and the cost of the final product is a key factor when determining the success of our product.

### 5.1 FINANCE AND BUDGETS

By producing a working prototype and performing design verification tests, some of the £ 1000 project budget was used for purchasing materials which were not used in the final product. This was planned for from the beginning of the project and careful project management ensured the project did not run over budget. Table 10 shows a breakdown of the total costs planned and the actual expenditure. The PQ-12 motors were responsible for budget in the motors/sensor category being exceeded; this was due to the motors being purchased from an ICIS approved supplier at a significantly higher price than they are obtainable for on the open market. The overall budget for the project, however, remained below the planned budget due to planning and accounting for this risk. In total, only £ 575 of the total budget was spent, making this project successful and cost efficient.

Table 10: Breakdown of Budget

Budget Breakdown:	Allocation:	Expenditure:
<b>Motors / Actuators / Sensors</b>	£250.00	£342.57
<b>Various Materials</b>	£150.00	£47.41
<b>Plastic Filament</b>	£100.00	£117.49
<b>Other Electronics</b>	£100.00	£67.50
<b>Total:</b>	£600.00	£574.97

### 5.2 FINAL PRODUCT COST

Table 11 shows the exact cost to manufacture the final prototype by summing the cost of all purchased and manufactured components. This was £ 399.02, however, if purchasing the product through non-ICIS suppliers, significant savings could be made by procuring the PQ-12 motors for far cheaper – bringing the total cost down to £ 238.73. The manufacturing methods necessary are also low cost, with only a budget 3-D printer (around £ 150) and a soldering station (around £ 10) required to manufacture the product.



Table 11: Final prototype cost

Product Name / Descriptor & (Purchaser)	Supplier	Unit Cost (incl. shipping)	Quantity / Portion of Packet	Total Cost	Budget Category
<b>Actuonix PQ12 Micro Linear Actuator, 20% Duty Cycle, 6V dc, 10mm/s, 20mm</b>	RS - Online	£113.03	3	£339.09	Motors / Actuators / Sensors
<b>Straps</b>	Amazon	£7.95	0.5	£3.98	Various Materials
<b>JST-PH Wire Assembly</b>	Pimoroni	£3.59	0.1	£0.36	Various Materials
<b>Wide Black Elastic Band</b>	Amazon	£4.99	0.1	£0.50	Various Materials
<b>Eventronic ET 1002 Heat Shrink Tubing Electric Insulation Heat Shrink Wrap Cable Sleeve 5 colours</b>	Amazon	£5.99	0.1	£0.60	Various Materials
<b>RS PRO 3.7V, Lithium Polymer Rechargeable Battery, 2 Ah</b>	RS - Online	£17.70	1	£17.70	Other Electronics
<b>LATEX FREE BRACES Elastic Orthodontic Bands</b>	Ebay	£2.99	0.1	£0.30	Various Materials
<b>ADAFRUIT Feather Cortex-M0 Proto Board</b>	RS	£15.21	1	£15.21	Other Electronics
<b>FeaterWing Latching Mini Relay Board</b>	RS	£6.07	1	£6.07	Other Electronics
<b>Short Feather Headers Kit 12-pin and 16-pin Female Header Set</b>	Pimoroni	£4.49	1	£4.49	Other Electronics
<b>All Printed Components</b>		-	-	£10.73	Plastic Filament
			<b>Total Cost</b>	£399.02	



## 6 TESTING AND DESIGN VERIFICATION

The third main component of this design, make and test project is, naturally, testing. This is a crucial part of the process, where the manufactured product is examined to discover if it meets the criteria specified in the PDS. As part of our iterative design process, many tests were performed at all stages of the project to inform design decisions, however, this section will only focus on the final tests performed to verify the product against the PDS.

### 6.1 DESTRUCTIVE TESTING

Destructive testing was performed, focussing on the mechanical strength of the product. Three tests were planned: a 3-point bent test to verify the maximum load; an impact test to evaluate toughness and robustness of the product; and a fatigue test to ensure the lifetime is not limited by fatigue issues.

---

#### 6.1.1 3-POINT BEND

---

##### 6.1.1.1 INTRODUCTION

As specified in section 4.3.1, 3-D printed components are anisotropic, meaning each component had different material properties and failure points according to its print orientation. To test the design, the stress and failure points needed to be quantitatively assessed using destructive testing. Therefore, an experiment was done to assess the strength of the device, specified in the PDS as minimum 50 N, and determine the failure criteria.

---

##### 6.1.1.2 METHODS AND DATA

In this experiment, three test samples of the working prototype were printed in PLA and placed onto a 3-point bend workpiece holding in an Instron tension and compression machine. The purpose was to test the strength of the connecting pins between the hand and the wrist and find the maximum theoretical load that the hand could hold, in order to verify the PDS condition of withstanding a 50 N load. There was a 35 mm distance from the centre to each support, and machine extended at a rate of 1 mm/s. The setup is demonstrated in Figure 34. The time, displacement and load were recorded. The specimen was compressed until the load dropped by 60%, which occurred after the specimen fractured. The data was analysed to find the maximum force applied before fracture, and the component visually inspected to find the point of failure. Using the maximum force applied, the maximum load applied to the end of the hand can be calculated by doing a force balance, then finding the resulting moment about the whole hand unit, given by Equation 4.



$$Max\ Load\ for\ Hand = \frac{Force\ Applied}{2} \times \frac{distance\ to\ pivot}{distance\ to\ end\ of\ hand} = \frac{F_a}{2} \times \frac{0.0035}{0.0075}$$

Equation 4





Figure 34 - 3-point bend set up

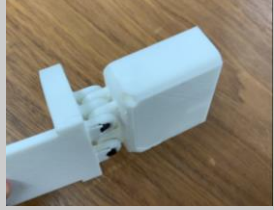
### 6.1.1.3 RESULTS

The results of this experiment are found below in Table 12.

Table 12: 3-point bend test results

Sample	Max Force Applied (N)	Max Load of whole hand (N)	Picture Failure Mechanism
1	336.7	78.6	
2	570.6	133	



3	524.8	122	
Average	477.4	111	Layer separation

---

#### 6.1.1.4 DISCUSSION

This data shows that the point of fracture of each sample was not the connecting pins between the hand and the wrist; the failure was layer separation, demonstrating that the connecting pins are strong enough to connect the two sections.

Moreover, the average maximum theoretical load that can be applied to the whole hand is 111 N, which is higher than the specified minimum load to failure of 50 N in the PDS. Thus, the test can be considered a success, and validates the stated PDS criterion.

---

#### 6.1.2 IMPACT TEST

To test the durability of the design a simple drop test was conducted. In this experiment the whole product was dropped from gradually increasing heights until a fracture occurred. The aim of this experiment was to ensure that the device would be resistant to being knocked, dropped and hit; this is important because many low cost designs do not have the durability and toughness to survive day to day usage. The results found that the maximum height the product could be dropped from is 2 metres and the failure mechanism was a fracture on the thumb connecting point, pictured in Figure 35. This test was considered a success, as 2 m represents a much greater height than any real-world drops are likely to occur at – this also shows a general durability as small impacts are unlikely to damage it.



*Figure 35: Close up of fracture point from drop-test*



---

### 6.1.3 FATIGUE TEST

This aspect of the project was unable to be completed due to the college shutdown caused by COVID-19. The details of this are properly discussed in section 7 (alternative work package) and the following paragraph explains the planned format of the test.

Fatigue testing was planned to verify the product life objective from the PDS (2 years minimum). The parts of the design most susceptible to fatigue are the fingers, so fatigue testing would have simulated many stress cycles by writing a program to open and close the fingers of the hand continuously over the course of several days. Once a specified number of cycles was complete, the fingers would be inspected for visible damage and a loading test would be performed to ensure the strength had not degraded due to fatigue.

### 6.2 GRIP STRENGTH TEST

An important aspect to test was the requirement that maximum grip force be  $\geq 30$  N. This could not be done analytically due to the complexities in modelling the various aspects of the system, so a practical test was required. 3.5 kg of items (weighed using a digital scale) were placed into a supermarket shopping bag, and a working prototype prosthetic (shown in Figure 36) was put into 'closed' grip mode, with the handles of the bag inside the grip. The prosthetic was then moved upwards (with force applied from the wrist unit, as it would be in reality), lifting the bag clear of the floor. It was then held in this position for sixty seconds. At the end of that period, there was no visible grip relaxation, extension of cabling, or any other indication that this weight was beyond the limits of the design.



*Figure 36: 3.5 kg lift demonstration with working prototype*



### 6.3 USER TESTING

Some of the most important tests planned were user tests, which would have commenced in three stages. First, members of this group would test the muscle sensing accuracy to verify that it can perform with 90 % accuracy as specified in the PDS. The second stage would involve inviting an amputee to test the device, with the goal of gathering more data about gesture recognition accuracy and to test how long it takes to learn to control the device (to compare against the 30 minutes goal set by the PDS). The final stage of user testing would involve an amputee using the prosthetic hand to navigate a specially designed, timed course such as the anthropomorphic hand assessment protocol developed by Llop-Harillo et al (38).

Unfortunately, these tests could not be performed due to practical project work being cut short by the early college shutdown – although it was possible to perform simulated tests to verify the 90 % accuracy of the device (further discussed in section 7, alternative work package).



## 7 ALTERNATIVE WORK PACKAGE

### 7.1 EFFECT OF EARLY UNIVERSITY SHUTDOWN ON PROJECT

The unprecedented shutdown of the college due to the rapidly developing pandemic situation (known as COVID-19) is an event which was not planned for by this group when considering risks to the project. The novelty and rapidly increasing severity of this event, combined with deadlines which were brought forward by several months, helped to create a landscape which was quickly shifting under our feet; the college shutdown adversely affected the project by cutting the available time to complete three project areas:

- ⚡ Fatigue testing of mechanical parts to verify product lifetime.
- ⚡ Transference of electronic components from working prototype to final prototype (this occurred in part but could not be fully completed).
- ⚡ Final testing of the completed prosthetic hand against some aspects of the PDS.

The source of disruption came from the aforementioned (multiple) deadline changes as well as one of our group (Charles) requiring spending the final week of the spring term self-isolating with suspected symptoms of the disease. This section details the estimated time which would have been required to complete the project as planned and explains the alternative work which was performed to account for this discrepancy, as well as modifications to planned directions of work to meet objectives where there was disruption due to the shutdown.

### 7.2 DETAILS OF UNCOMPLETED TASKS

We estimated that there were approximately 15 hours of work left, which was agreed as realistic by our supervisor, broken down as follows:

- ⚡ 4 hours for fatigue testing (2 hours for 2 group members).
- ⚡ 6 hours for soldering of final product and any associated debugging or minor coding changes to improve user experience (3 hours for 2 group members).
- ⚡ 5 hours for user testing and any other necessary tests to confirm performance (2.5 hours for 2 group members).

This group considers itself fortunate in that such a relatively minimal amount of work was cut off in these circumstances. However, the loss of the user testing component is disheartening.





### 7.3 DETAILS OF ALTERNATIVE WORK PACKAGE

After discussion with Dr Vaidyanathan, it was decided that the alternate work package would consist of two components: muscle sensing testing (performed in a simulated environment) and a brief discussion of potential changes to the product had mass manufacturing been chosen as the preferred production method.

The muscle sensing component was chosen because the inability to perform end user testing was a significant blow to the project. By performing simulated tests, we hope to prove that the final product (had we been able to complete it) would perform according to the 90 % gesture recognition accuracy parameter set out in the product design specification. Conversely, the second component of the alternative work package (mass manufacture discussion) was chosen to give us an opportunity to explore this area of design and manufacture. Fundamental to the project from the start was the concept that it could be developed using low-volume distributed manufacturing methods such as additive manufacturing; by making a plan for the product to be mass manufactured, we can explore the differences in design that might have occurred, had the project been focussed on mass manufacture from the start.

### 7.4 ALTERNATIVE WORK

Manually sorting through raw data, writing new testing software and collecting and analysing results for the simulated muscle testing took 1 group member approximately 8 hours, so this component of the alternative work package makes up for 53 % of the work practical work missed due to college shutdown. The design for mass manufacture section consisted of research and retroactively considering possible design changes with mass manufacture in mind – this took two group members approximately 3.5 hours each, making up the remaining 47 % of work missed due to COVID-19.

---

#### 7.4.1 SIMULATED MUSCLE SENSING TESTING

---

##### 7.4.1.1 INTRODUCTION

Fortunately, despite the college shutdown and the earlier than anticipated product hand-in, raw MMG data (collected from earlier tests as part of our iterative design process) was available for use in testing. This meant that it was possible to verify the muscle sensing accuracy of the prosthesis by writing new software that takes this raw input data and simulates the action of the real device. The primary goal of these tests was to verify that the device can achieve the 90% gesture recognition accuracy set out in the PDS.



---

#### 7.4.1.2 METHODS AND DATA

The available raw data consisted of text files containing timestamped readings from an Arduino UNO analogue to digital converter when connected to a single MMG sensor – each of these files consisted of 10 seconds of signal, labelled with the muscle the sensor was recording from and the movement attempted. Immediately some of the data had to be discarded, due to poor signal quality or inconsistent sampling rate (which was an issue with some of the earliest implementations of the data acquisition software), leaving 17 sets of usable data. These datasets included readings from all 6 muscle groups identified as viable in section 3.5.1, so cover a wide range of different possible use cases. 10 of these sets involved recording the muscle whilst performing the ‘target movement’ (for example the biceps brachii in elbow flexion), whereas 7 of the datasets were recorded during a ‘distraction movement’ (such as the biceps brachii during shoulder rotation). This is important because it allows the experiment to determine the ‘false positive’ rate of the device (also known as type I errors) – in this context, a type I error is where the prosthesis registers a distraction movement as an intentional muscle contraction, as opposed to ignoring it.

Software was written in Python to extract the data from the text files and process it using the same signal processing and classification algorithm detailed in section 3.5.2. The output from this script showed whether, had the test been performed by a real user, the prosthesis would have actuated; this output was then cross referenced against the known muscle movement when performing the test to see if the device would have actuated correctly. This is demonstrated in Figure 37, where the device correctly identifies a three second isometric contraction of the brachioradialis muscle.

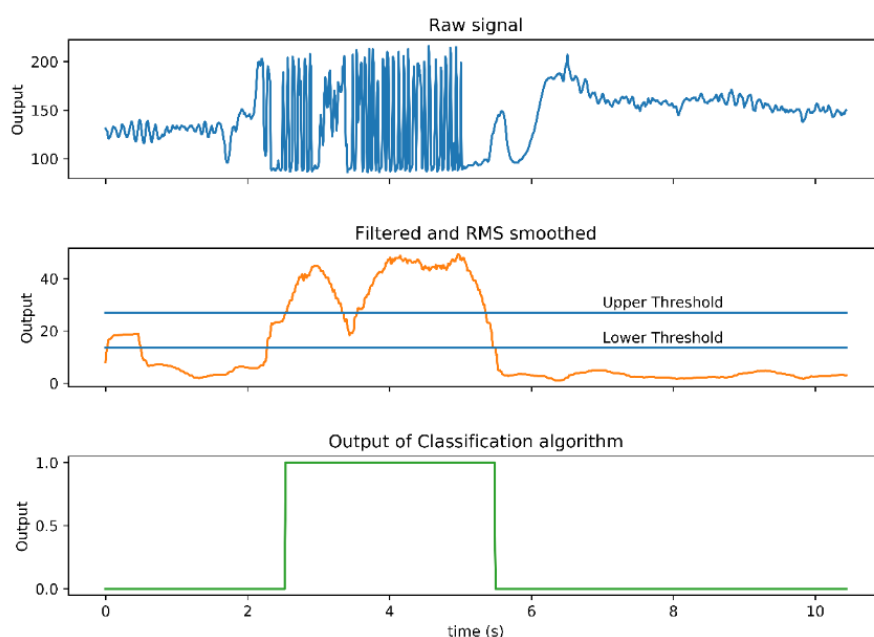


Figure 37: Simulated device output for a 3 second isometric brachioradialis contraction



One fundamental difference between the simulated test and the real-life testing that was planned is that a real user would tune the threshold value of the classification algorithm to their preferences before starting the test, however there is no data that we can use to determine this for the simulated test. For this reason, the simulated testing was repeated over a range of possible threshold values to provide data about how the prosthesis would have performed if it were set up correctly. This also allows us to understand how sensitive the device is to operation at non-optimal setups.

### 7.4.1.3 RESULTS

Figure 38 shows the full results from the simulated tests, with information about the accuracy rate – defined as the percentage of the time that the device performs as intended (either correctly identifying an intentional contraction or correctly ignoring a distraction contraction). Information is also displayed about the rate of type I and type II errors (false positives and false negatives respectively).

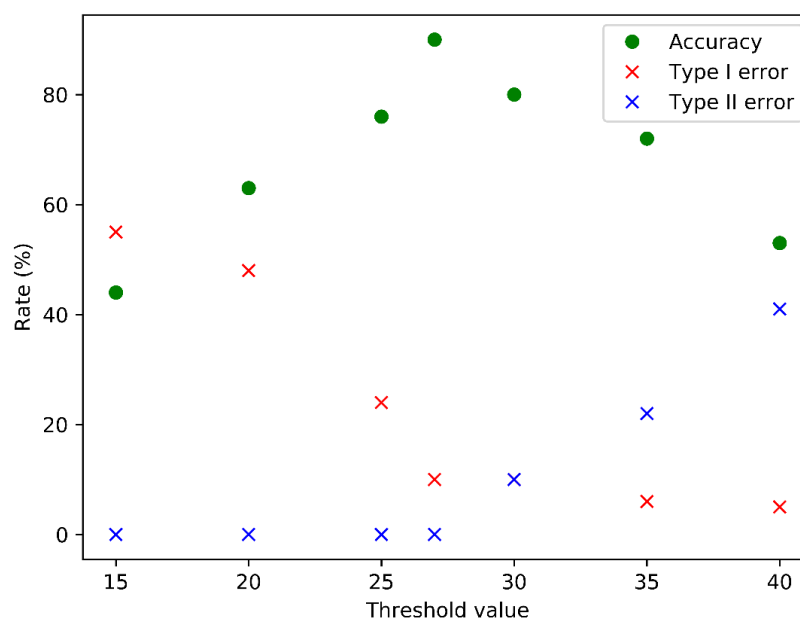


Figure 38: Results from simulated testing

The results show that, at the optimal threshold value for this individual, the device reaches a maximum accuracy of 90 %. There is a small window of threshold values around this point where the accuracy remains in the region of 75 - 80 %, however the accuracy begins to drop off sharply outside this range. Predictably, at low threshold values, type I errors dominate whereas, at high threshold values, type II errors dominate.



---

#### 7.4.1.4 DISCUSSION

These results are promising because they imply that, if the user sets up the device properly, they can achieve the 90 % accuracy that the PDS requires. However, we should remain tentative about these results because the virtual experiment described here carries a host of potential sources of error and inaccuracies – so the results are much less valuable than those which would be attained from a real user trialling the finished product.

Arguably the most significant limitation of the simulated testing is that the available data was collected using only a single MMG sensor. Since the final product has two sensors, there is a possibility of cross-noise, where signals from one sensor are detected by the other – unfortunately, this testing method was unable to investigate this prospect. This problem combined with the low amount of available data (only 17 datasets) severely limits the validity of the simulated experiment performed. However, this group believes that despite the known issues, the experiment was successful in demonstrating the ability of the device to accurately classify muscle movement and provides at least some evidence that it can perform to the 90 % accuracy standard set out in the PDS.

---

#### 7.4.2 DESIGN FOR MASS MANUFACTURE

From the start, this project was planned with low-volume, distributed manufacturing in mind and the product was designed such that, theoretically, any 3-D printing hobbyist would be able to manufacture and assemble the device by downloading the CAD files and software online. However, if this product had been intended to be circulated to the global market on an industrial scale, mass manufacturing would unquestionably be a design consideration and, in this scenario, the final product would almost certainly be different to our solution. This section explores different types of mass manufacture relevant to a product of this type and what, if any, design changes would be necessary to adapt our product for mass manufacture. The advantages and disadvantages of this change in manufacturing method are also considered.

*Most of the product as is consists of FDM 3-D printed PETG, for which there are many mass-manufacturable alternatives.*

Table 13 identifies the most suitable methods, lists some advantages and disadvantages and notes the design changes necessary to use them.



Table 13: Comparison of mass manufacturing methods suitable to replace 3-D printed PETG

Manufacturing method	Advantages	Disadvantages	Changes required to current design
<b>Compression Moulding</b>	Simple, and can be used with long fibre reinforcements which could increase uniaxial or biaxial strength.	Somewhat expensive, and as thermosets would be used, the process would be slow due to the curing time required.	As thermosets would need to be used (compression moulding can work with polymers, but only expensive high-performance ones), new materials with similar or better properties to ABS and PLA would need to be selected. Furthermore, thermosets do not show a brittle-to-ductile change at their glass transition temperature $T_g$ , so a new wrist unit shaping method would be needed (the current design of heat moulding to an amputee's stump would not be possible).
<b>Injection moulding</b>	Very cheap per part, and good surface quality.	High start-up costs from machine and mould, and some manufacturing defects possible.	There are no apparent changes that would be required for the design. Care would be needed in regard to gate placement to limit weld lines and points of weakness in the product.
<b>Reaction Injection Moulding (RIM)</b>	Much lower start-up costs than injection moulding due to simple design, and it being a low-pressure process.	Slightly slower due to curing times.	RIM is another process for thermosets, so would require the same design modifications as identified for 'Compression moulding'.
<b>Selective Laser Sintering (SLS)</b>	Faster and gives better surface finish compared to Fused Filament Fabrication (FFF)	Relatively high cost, and similar structural issues that come with 3-D printing compared to FFF.	SLS is an alternative form of 3-D printing, using highly concentrated lasers to melt particles together, layer by layer. Alternative polymers would have to be selected, as SLS is usually only suitable for polymers such as polyamide or polystyrene – if selected carefully however, no further changes would be required for the wrist and hand units.

Injection moulding is likely to be the most suitable mass manufacturing technique to replace 3-D printed PETG due to the cost advantages it presents. No major design changes would be required to manufacture this using injection moulding as the geometry of the current parts allows them to be made using standard injection moulding procedure.

*The outer casing for the fingers, however, is made from a 3-D printed TPU structure (also using FDM methods), with only 10 % infill for flexibility. This would be impossible to replicate using any of the methods mentioned in*



Table 13 so if FFF was not deemed suitable for a mass-manufacturing scale, perhaps due to its speed, cost or precision, there would have to be a completely new design – such as replacing them with a silicone rubber ‘skin’ containing a similar solid core.

There are also some other advantages that would come with mass manufacturing:

- ⚡ It would be cost-effective to make a custom circuit board, reducing the cost of electronics components and the size that the electronics would take up, allowing for a sleeker design or greater battery capacity.
- ⚡ Due to the economies of scale concept, centralised manufacturing (and purchasing) would inevitably lead to a potentially significant reduction in materials and electronic costs per product

In summary, mass manufacturing is achievable without significant modifications to the design of the product. It would allow cost savings from a number of directions, but would naturally reduce the customisable nature of the designs and how easily they could be repaired or replaced, and would only be economically sensible if there was a suitably large customer base (tens of thousands per annum, if not more). Naturally, having centralised production (as opposed to making the 3-D print files open source and simply selling the software and electronic components) and selling a pre-packed, hassle-free product would also allow a greater mark-up to be applied and thus a higher profit margin generated - if this was being considered as a money-generating operation rather than done at or near cost.



## 8 DISCUSSION

This section discusses the successes and failures of this project, consisting of three parts: evaluation of the product against the PDS, a general discussion and a brief discussion of potential avenues for future work.

### 8.1 PDS EVALUATION

The product design specification lists 19 quantifiable objectives (with various levels of associated importance) for the project and sets out appropriate tests to ensure that each of them is met. This section uses these tests to evaluate the performance of the final product against the performance envisaged in the PDS and expands upon the notable tests and results.

Table 15 displays the PDS, but with a colour coded verification column: green cells represent tests which were completed, where the product successfully fulfilled the criteria; blue cells represent tests which could not be performed due to the college shutdown response to COVID-19, however, suitable alternative tests were identified and performed; and red cells represent tests which could not be performed due to COVID-19, with no suitable alternatives. Table 14 is a reference table to simplify the colour coding convention.

*Table 14: Meanings of the colour-coding convention in the PDS*

	Green	Yellow	Blue
Aspect	Crucial	Important, but based on arbitrary objective	Non-critical
Verification	Successfully verified by testing	Alternative test performed due to COVID-19	Test not performed due to COVID-19





Table 15: PDS including verification performed

	Aspect	Objective	Justification	Verification
Performance	Number of grip poses*	$\geq 3$	Three poses should provide sufficient functionality for key uses in daily life.	Design review.
	Maximum grip force	$\geq 30$ N	30 N is suitable for basic daily tasks such as carrying shopping and shaking hands.	Prototype testing using force meter. Lifted 3.5 kg for 60 seconds without any visible issues (see 6.2).
	Sensing method	MMG	MMG sensing will be used for signal acquisition.	Design review.
	Gesture recognition accuracy	90 %	For the device to be useable daily, it must correctly actuate 90 % of the time to avoid user frustration.	Simulated muscle sensing testing (see 7.4.1).
	Battery life	12 hours	12 hours of continuous use would last through a full workday and use at home.	Current draw calculations (see 3.6.4.1).
Life	Product lifespan	2 years	Operate for a minimum of 2 years before failure under standard use.	Fatigue testing of prototype.
	Waterproofing	IP33 rating	This should allow for protection from splashes and small solid objects.	Test prototype against standards.
Size	Form factor	Adult sized right hand	The device should fit adult transradial amputees. A basic socket will also be designed for demonstration purposes, although this is not the focus of this project.	Design review. Hand is 193.4 x 65.6 mm, smaller than the adult average (39).
	Mass	< 500g	An average human hand has a mass of approximately 500g. This should therefore be a reasonable upper limit for the product mass, to avoid user discomfort.	Weigh prototype with digital balance. Confirmed as 468 g.
Safety	Maximum electronics temperature	< 40 °C	Skin-contact and external surface temperatures must remain under 40 °C to avoid potential discomfort and burns (based on ASTM C1055 standards (27)).	Run for 10 mins then scan with infrared thermometer.
	Transmission enclosure	Enclosed	Transmission parts should be enclosed for the user's safety.	Design review.
	Electronics enclosure	Enclosed	Electronics should be enclosed to minimise the chances of burns and shocks.	Design review.
	Loading	$\geq 50$ N	The mechanism must not break when overloaded.	Perform loading test on prototype. Maximum load before failure was tested as 111 N (see 6.1.1).
Production	Quantity	$\geq 2$	An initial working prototype will be made followed by a final product.	Count prototypes.
	Cost*	< £400	If the final device has a materials cost of less than £400, it will be accessible to users with a wide range of economic circumstances.	Summing cost from bill of materials. £399.02 using ICIS providers (see 5.1).
	Materials*	Cheap and widely available materials	Material selection will occur at a later project stage and will be intertwined with the manufacturing processes chosen.	Design review.
	Processes	3-D printing and related methods	The product must be manufacturable by volunteer hobbyists and engineers using methods reasonably accessible to them.	Design review.
	Assembly	< 3 hours	Must be assembled and fitted to an amputee in less than three hours by an engineer.	Timed test with stopwatch.
	Training	<30 mins	Users should be able to learn the basics of controlling the system quickly to avoid frustration.	Timed test with stopwatch.



From inspection of Table 15, it is clear that 12 of the 19 objectives were tested and successfully verified, with 9 of the 10 ‘crucial’ aspects being successfully tested. 5 tests were, regrettably, unable to be performed at all due to COVID-19 and 2 tests were performed, but in a different way to what was envisaged in the PDS (again, due to COVID-19).

---

#### 8.1.1 SUCCESSFUL TESTS

Of the successful tests identified in Table 14, the most significant were the maximum grip force and maximum loading tests. These have been described in full in section 6 and demonstrate that the product has exceeded the criteria set out in the specification. This is extremely promising because it shows the strength and durability of this product – factors traditionally lacking from attempts to design low-cost prosthetic devices.

---

#### 8.1.2 ALTERNATIVE TESTS

Two notable tests are the alternative tests carried out in lieu of those that were planned. The first is the simulated muscle sensing test, described in section 7.4.1. This test, despite its limitations, proved that the device can provide high accuracy muscle sensing when correctly set up. This is one of the most significant results in this project due to the evidence it provides that MMG sensing can provide accuracy on par with EMG, which is typically considered the gold standard. The other alternative test performed was the battery life testing, which was verified by calculation instead of practical testing. The calculations performed are detailed in the electronic design section (3.6.4) and demonstrate that, even with conservative assumptions, the battery should last for the 12 hours specified with a safety factor of 1.3. These calculations combined with their generous margin for error give us confidence that the product will perform with sufficient battery life.

---

#### 8.1.3 TESTS WHICH COULD NOT BE PERFORMED

Only one of the five tests not performed pertained to a critical aspect of the PDS. This was the maximum operating temperature requirement and is important to be verified for safety of the product. Although the test was not performed, no concerns were raised about temperature when operating the functional prototype; this admittedly anecdotal evidence suggests that the device was likely to pass the test, had it been possible to perform it.

---

### 8.2 GENERAL DISCUSSION

This project was self-proposed so it was difficult to accurately gauge a project scope which would allow for lots of development without being unrealistic. We believe that we erred on the ambitious



side, with difficult targets set out in the brief (section 1.1), substantiated by a stringent PDS and this group believes that the final product meets all these ambitious targets, having produced a low-cost, 3-D-printable device capable of multiple pre-set grips controlled by MMG sensors to an analytically proven accuracy of 90%. The final cost of the prototype was £399.02 using ICIS providers, and can be built for a cost of just £238.73 using preferred suppliers. Detailed planning and project management helped us to meet these tough targets and ensure that the project was completed efficiently and effectively and helped us to mitigate and overcome the adverse effects of COVID-19 on this project.

The following sections will qualitatively discuss the benefits and failures of certain aspects of the design and process.

---

### 8.2.1 MECHANICAL DESIGN

Expert advice, given by Alex Lewis and Liang He, helped shape the project from the start by bringing us to understand user needs. This helped us to focus the device on function rather than form and ensure that durability and strength were at the forefront of mechanical design. By using an iterative design process centred around rapid 3-D printing of prototypes, we performed many small cycles of design, make and test throughout this project – helping to refine parts and gain insight where analytical calculations may have failed. Upon reflection, this design philosophy was extremely effective and was a key factor in the success of the project.

---

### 8.2.2 SOFTWARE AND CONTROL

One aspect of this project which was underestimated at the beginning would be the difficulty of developing effective software which fulfils the performance criteria specified in the PDS. Reaching the final stage of the software required learning about digital signal processing (a significant topic in its own right), as well as improving our knowledge of the C programming language and computer science topics such as big 'O' notation and program optimisation. The unanticipated difficulty of this part of the project provided some frustration, however, was ultimately rewarding – with the final algorithms coming to fruition as a result of iterative experimentation, reading related literature and learning about topics related to computer science and electrical engineering.

---

### 8.2.3 ELECTRONICS

Electronic design was another topic more complex than initially appreciated, with trade-offs between design complexity, size and functionality forcing difficult choices to be made and solutions to be conjured. Ultimately, the electronic design was a success, with the electronics able to tie together the mechanical and software components into a device capable of meeting all relevant PDS



requirements. The 12-hour battery life and over 3 kg grip force were particular successes, especially when considering the compact form factor of the final product. The decision to not design a printed circuit board (PCB) to house all the electronics was a wise one as it would have created significant extra work, however, we expect that this would need to be done before the product could be launched commercially.

---

#### 8.2.4 PRODUCT PRICE POINT AND ACCESSIBILITY

The brief and specification set out the goals that the product must be manufacturable by volunteer engineers or hobbyists at a low price point (set as £ 400). The final product was manufactured for a cost of £ 399 and we estimate that it could be reproduced using non-ICIS suppliers for £ 239. We believe that this is a major success of this project, given that this device is designed to compete with products starting at £ 10 000. The only tools required to reproduce our product are a suitable 3-D printer (roughly £ 150) and a soldering station (roughly £ 10) so it is certainly feasible that there are many engineers and hobbyists with suitable equipment to manufacture this device. In fact, an individual would theoretically be able to purchase all required materials, including the printer, and manufacture ATLAS completely from scratch for an order of magnitude less than any other electronic prosthetic hand currently on the market. There was one barrier to accessibility for this project, however, which is the reliance on the proprietary MMG microphones that SERG technologies kindly gave us. The raw materials cost for these sensors is estimated to be around £ 5 so this should not be too great a barrier as, with a little extra work, open-source sensors could be designed to accompany this project.

---

#### 8.2.5 ALTERNATIVE WORK

Due to the unprecedented shutdown of the college due to the advent of COVID-19, certain aspects of the final prototype were unable to be completed in full, as discussed in detail in section 7. This primarily involved the transference of electronic components from the working prototype to the final prototype to complete a fully functioning final product. It also meant that certain PDS tests (7 tests) could not be completed to verify these aspects of the design. This was disappointing as it prevented the design from being fully validated – however, using alternative methods of assessment, two more tests were performed: the simulated muscle sensing tests and the analytical battery calculations. These virtual tests enabled 14 out of 19 PDS elements to be met. The remaining 5 elements would require further testing, although reasonable assumptions and anecdotal evidence allow us to infer that most of these tests would likely be passed. The fact that no PDS elements were



failed is absolutely considered a success, particularly when considering the ambitiously high bar set for many of the requirements.

The other part of the additional work package was an analysis of mass manufacture methods, with an eye to the design changes that would be required for the product to be mass manufactured. This finds that much of the design is injection-mouldable with no design changes required, however, the TPU sleeve over the fingers would require a redesign.

### 8.3 FUTURE WORK

Although this project succeeded in developing a low-cost, functional, MMG-controlled prosthetic hand and met the key aims specified in the project brief – there are several areas in which future development should occur if this product is to be taken to market. These areas include functionality, user interface and manufacturability; future work would likely hinge around, either in full or in part:

- ✦ Design of a printed circuit board to house the electronics in a more compact, pre-made package which could simply be slotted into the hand by volunteer makers.
- ✦ Design of our own MMG sensors, so we are not reliant on proprietary technology.
- ✦ End user testing by amputees, incorporating their feedback into the user interface.
- ✦ Introducing haptic feedback into the product to give users a tactile experience when grasping.
- ✦ Making fingers touch-screen compatible.
- ✦ More effective socket design for better suspension and to enable use by transhumeral amputees and people with wrist disarticulation amputations (estimated to account for 16 % and 2 % of upper limb amputations respectively (40)).
- ✦ Internet of things connectivity, allowing the amputee to control smart appliances with muscle movements.

These topics could be tackled as a future DMT project, by researchers or simply by volunteers who wish to develop this project into an open source commercial product which can be used in the near future by real amputees.



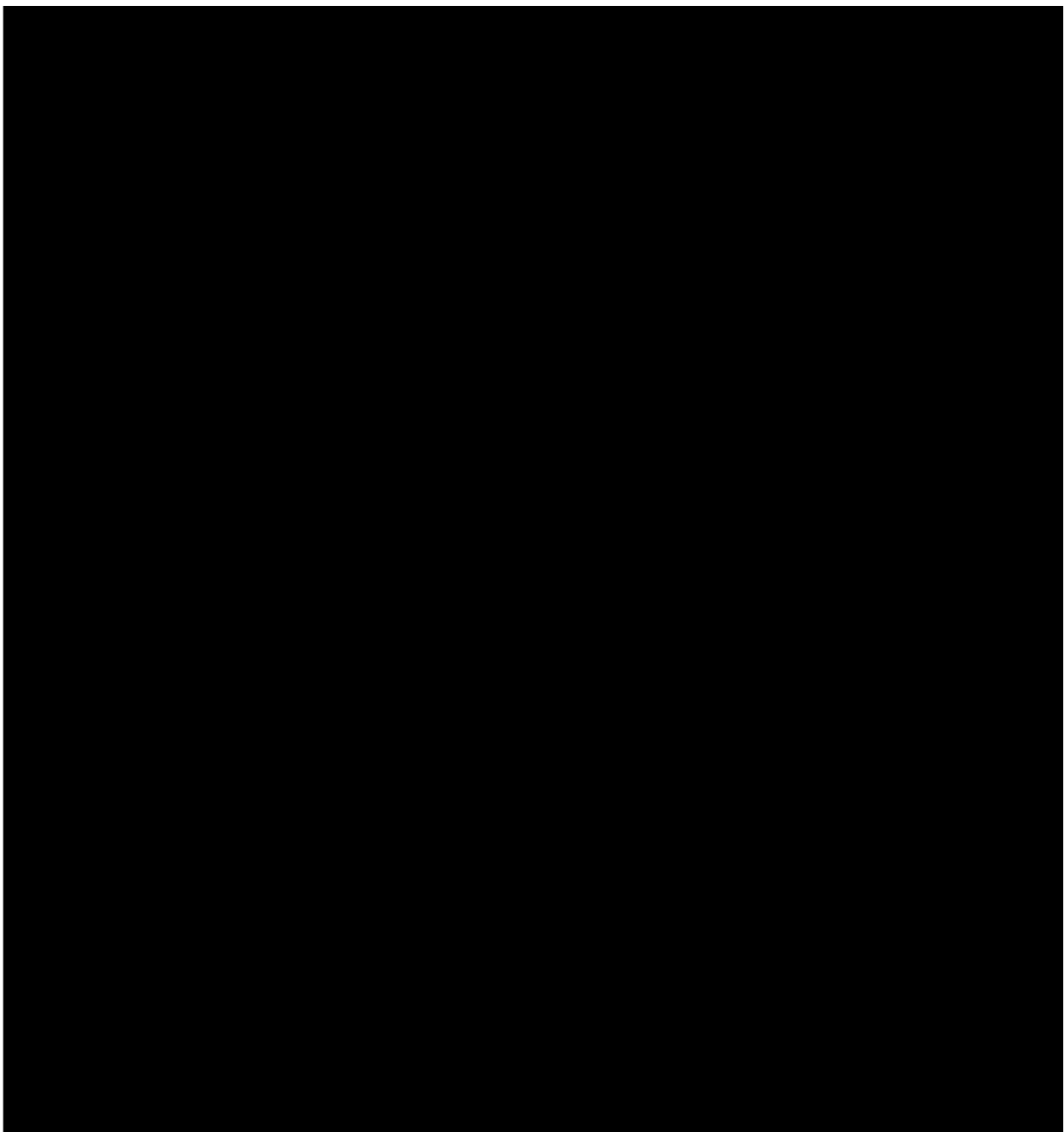
## 9 CONCLUSIONS

The aims at the start of this project were to create a low-cost MMG-controlled prosthetic hand, capable of several electro-mechanically operated grip patterns. The ATLAS design is a 3-D printed solution costing just £238.73, with three selectable grip patterns controlled by two arm-mounted MMG sensors. It has been designed for decentralised production, with elements of biomimicry including soft-hard composite fingers mirroring human biology, and various additional aspects built in including a rechargeable battery and a battery monitoring system, and an adjustable sensitivity level to make the product accessible to a wider range of users. It is considered to have met all the aims initially set out and exceeded them in some areas. One of the most novel aspects of this project was the development of an MMG control system, something which is not seen in any devices currently on the market. The benefits of EMG over MMG (and vice-versa) have been discussed at length in this report, but in summary we believe that this project has demonstrated MMG is a suitable method of prosthetic control, at least on par with EMG, with high accuracies of up to 90% demonstrated when correctly tuned. Covid-19, and the associated early shutdown of Imperial College London, had several frustrating impacts on the project, including the prevention of the final prototype being fully assembled and demonstrated as functional. However, all core concepts of the design were demonstrated in the working prototype and analytical testing, with 14 of 19 product design specifications met and proven. While it has been acknowledged that this product would require further development before it could be released as a market-worthy product, we believe it provides a strong platform for further work and shows that a robust MMG-controlled prosthetic capable of several functional grips, which can be produced for an order of magnitude lower cost than the retail value of the cheapest EMG products on the market at present is not just a hypothetical possibility but a demonstrated and proven one.



## 10 PERSONAL REFLECTIVE REVIEWS

### 10.1



### 10.2 CHARLES JONES

Proposing this project, I believed that working in this area would give me the chance to delve into some of the areas of engineering that I enjoy that have only briefly been touched upon in the Mechanical Engineering course up to this point. I was excited to learn, so dived head-first into topics such as digital signal processing, software design, prosthetic device design and more. This wide-eyed optimism was perhaps naïve, as I soon began to understand the sheer depth of these topics and it



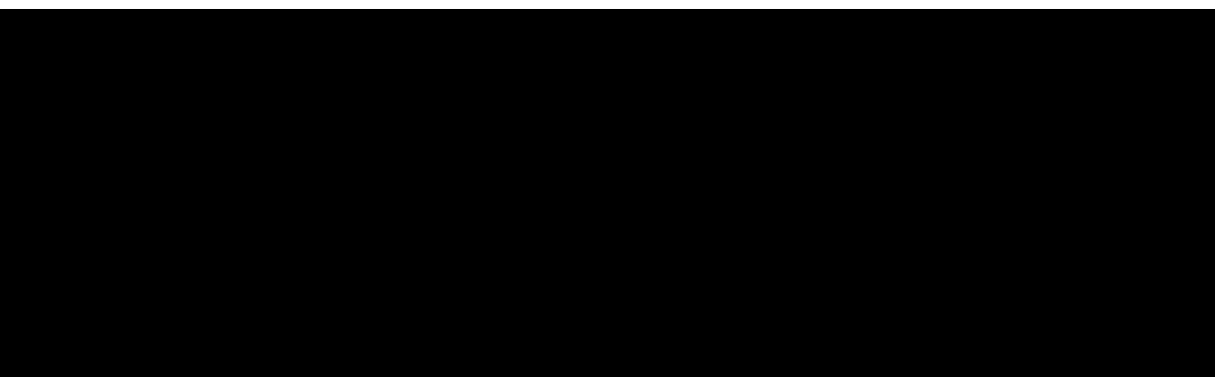


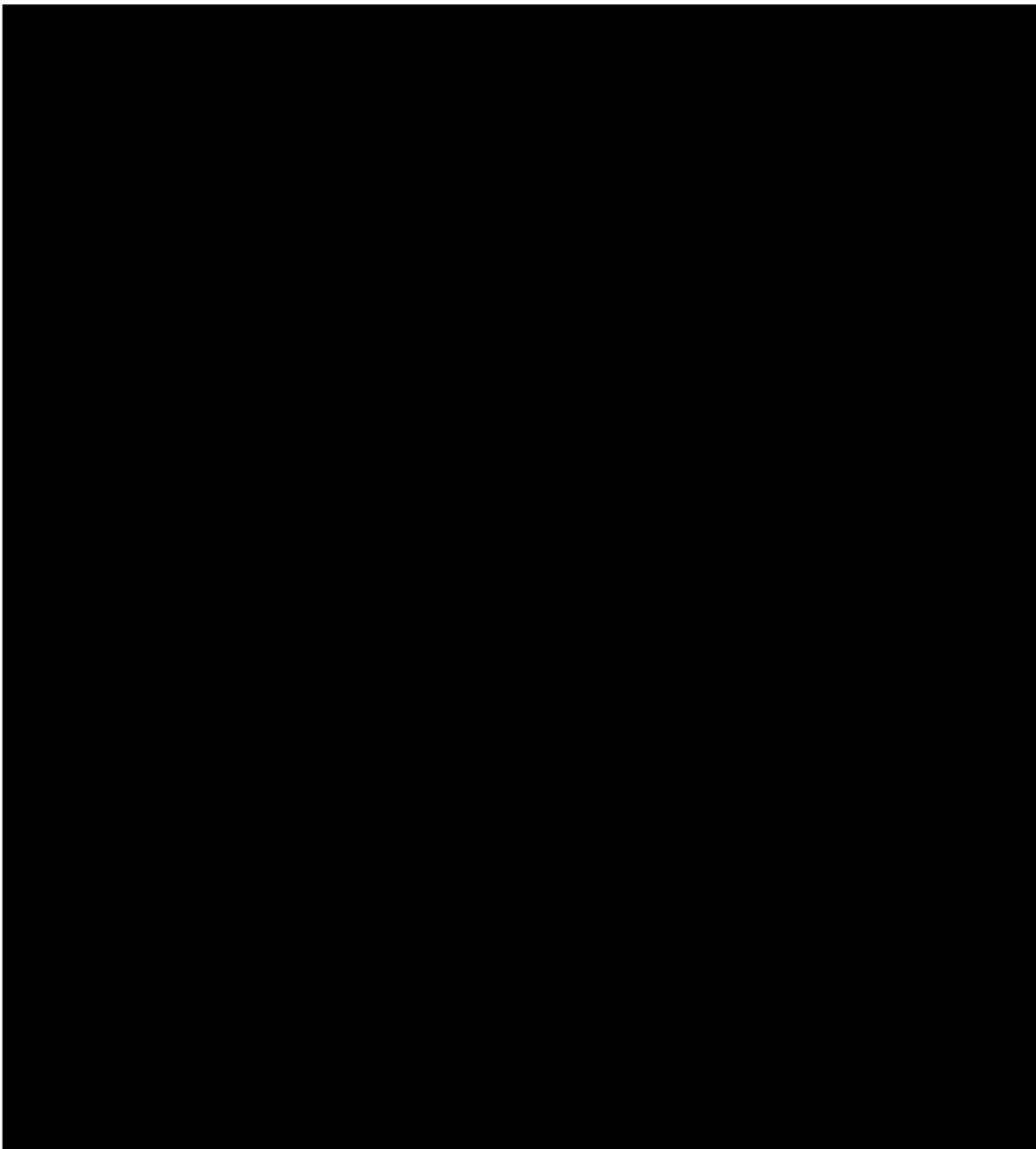
became clear that I was not going to master them in a single university project. Working on my literature research project this year, however, helped prepare me for this eventuality as I developed an important skill: the ability to critically read and digest vast amounts of content. Armed with this new tool, I began to break the back of these topics and the naïve optimism gave way to something more valuable – a genuine understanding of certain subjects and, more importantly, a general overview about what I did not know.

My role in this team was to develop software for the product which could enable accurate MMG muscle sensing and control. This was developed independently of and in parallel with much of the rest of the project, so in a lesser group, I might have felt isolated and unsupported in this role. I am happy to say that this was not the case, as excellent project management and a strong collaborative spirit within the group meant that I could assist with other parts of the project and receive assistance when I needed it. In future group projects, I will be sure to remember this point and to promote an environment where collaboration is central, and people feel supported in their roles. I will also try to be more realistic about goals from the start and will consult with experts to gauge the difficulty of different aspects of the project work.

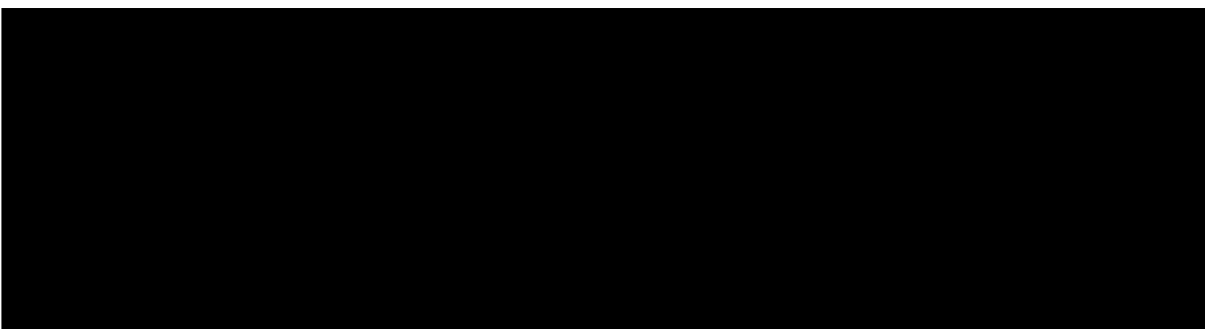
Throughout my experience of engineering projects, I have found that seeing the final product in action is the most satisfying part of the process, with all the hard work and toil being vindicated by the ability to show off a well-designed product. It is unsurprising then that I am disappointed that this feeling was robbed by the unfortunate and exceptional circumstances caused by the coronavirus pandemic. Despite this, I feel I can be proud of what we have achieved as a group – producing a final product which meets and exceeds the ambitious PDS we produced and could potentially act as a platform for others to develop a product which is of use to real amputees.

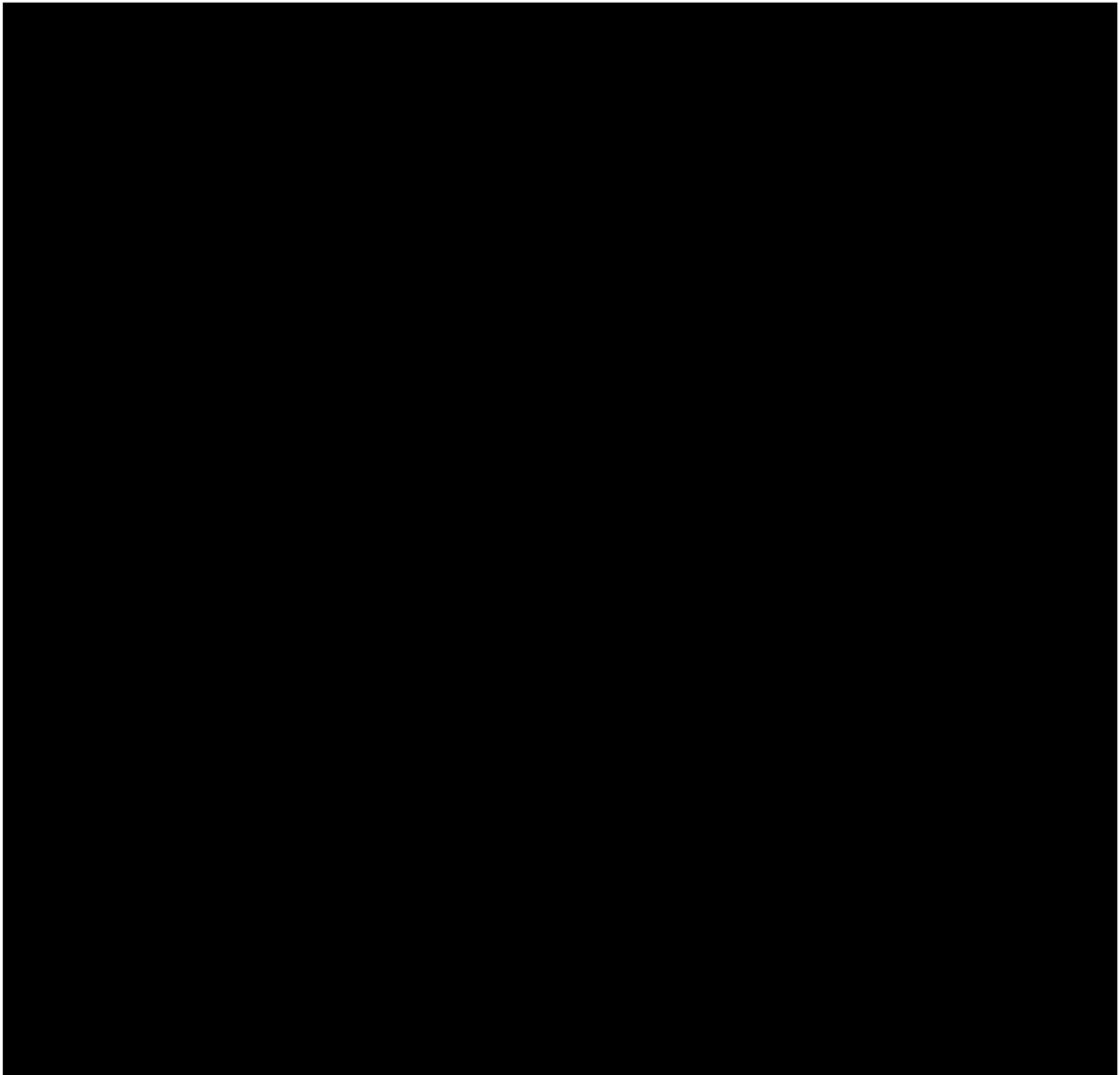
10.3





10.4





## 11 REFERENCES

- (1) Elkoura G, Singh K. Handrix: Animating the Human Hand. *Eurographics/SIGGRAPH Symposium on Computer Animation (2003)* Eurographics/SIGGRAPH Symposium on Computer Animation (2003), 2003. Toronto; 2003.
- (2) Cuccurullo SJ. *Physical Medicine and Rehabilitation Board Review*. 3rd ed. New York: Demos Medical Publishing; 2015.
- (3) Soyer K, Unver B, Tamer S, Ulger O. The importance of rehabilitation concerning upper extremity amputees: A Systematic Review. *Pakistan journal of medical sciences*. 2016; 32 (5): 1312-1319. Available from: doi: 10.12669/pjms.325.9922 Available from: <https://www.ncbi.nlm.nih.gov/pubmed/27882044> .
- (4) Atkins DJ, Heard DCY, Donovan WH. Epidemiologic Overview of Individuals with Upper-Limb Loss and Their Reported Research Priorities. *JPO: Journal of Prosthetics and Orthotics*. 1996; 8 (1): 2–11. Available from: [https://journals.lww.com/jpojournl/Abstract/1996/00810/Epidemiologic\\_Overview\\_of\\_Individuals\\_with.3.aspx](https://journals.lww.com/jpojournl/Abstract/1996/00810/Epidemiologic_Overview_of_Individuals_with.3.aspx) [Accessed May 28, 2020].
- (5) Cordella F, Ciancio AL, Sacchetti R, Davalli A, Cutti AG, Guglielmelli E, et al. Literature Review on Needs of Upper Limb Prosthesis Users. *Frontiers in neuroscience*. 2016; 10 209. Available from: doi: 10.3389/fnins.2016.00209 Available from: <https://www.ncbi.nlm.nih.gov/pubmed/27242413> .
- (6) Bicchi A. Hands for dexterous manipulation and robust grasping: a difficult road toward simplicity. *IEEE Transactions on Robotics and Automation*. 2000; 16 (6): 652-662. Available from: doi: 10.1109/70.897777 [Accessed May 28, 2020].
- (7) Davidson J. A survey of the satisfaction of upper limb amputees with their prostheses, their lifestyles, and their abilities. *Journal of Hand Therapy*. 2002; 15 (1): 62-70. Available from: doi: 10.1053/hanthe.2002.v15.01562 Available from: <http://dx.doi.org/10.1053/hanthe.2002.v15.01562> .
- (8) Heger H, Millstein S, Hunter GA. Electrically powered prostheses for the adult with an upper limb amputation. *The Journal of Bone and Joint Surgery. British volume*. 1985; 67-B (2): 278-281. Available from: doi: 10.1302/0301-620X.67B2.3980541 Available from: <https://doi.org/10.1302/0301-620X.67B2.3980541> .
- (9) Hameed HK, Hassan WZW, Shafie S, Ahmad SA, Jaafar H. A Review on Surface Electromyography-Controlled Hand Robotic Devices Used for Rehabilitation and Assistance in Activities of Daily Living. *JPO: Journal of Prosthetics and Orthotics*. 2020; 32 (1): 3–13. Available from: doi: 10.1097/JPO.0000000000000277 Available from: [https://journals.lww.com/jpojournl/Abstract/2020/01000/A\\_Review\\_on\\_Surface\\_Electromyography\\_Controlled.2.aspx](https://journals.lww.com/jpojournl/Abstract/2020/01000/A_Review_on_Surface_Electromyography_Controlled.2.aspx) [Accessed May 28, 2020].
- (10) Weir RFF, Troyk PR, DeMichele GA, Kerns DA, Schorsch JF, Maas H. Implantable Myoelectric Sensors (IMESs) for Intramuscular Electromyogram Recording. *IEEE transactions on bio-medical engineering*. 2009; 56 (1): 159-171. Available from: doi: 10.1109/TBME.2008.2005942 Available from: <https://www.ncbi.nlm.nih.gov/pmc/articles/PMC3157946/> [Accessed May 28, 2020].



(11) Atique MM, Rabbani S. A Cost-Effective Myoelectric Prosthetic Hand. *JPO: Journal of Prosthetics and Orthotics*. 2018; 30 (4): 231–235. Available from: doi: 10.1097/JPO.0000000000000211 Available from:

[https://journals.lww.com/jpojournl/Abstract/2018/10000/A\\_Cost\\_Effective\\_Myoelectric\\_Prosthetic\\_Hand.10.aspx](https://journals.lww.com/jpojournl/Abstract/2018/10000/A_Cost_Effective_Myoelectric_Prosthetic_Hand.10.aspx) [Accessed May 28, 2020].

(12) Ku I, Lee GK, Park CY, Lee J, Jeong E. Clinical outcomes of a low-cost single-channel myoelectric-interface three-dimensional hand prosthesis. *Archives of Plastic Surgery*. 2019; 46 (4): 303-310. Available from: doi: 10.5999/aps.2018.01375 Available from:

<https://www.openaire.eu/search/publication?articleId=od267::00f28fd89e80085e55b8e37b66699c15> [Accessed May 28, 2020].

(13) Sreenivasan N, Ulloa Gutierrez DF, Bifulco P, Cesarelli M, Gunawardana U, Gargiulo GD. Towards Ultra Low-Cost Myoactivated Prostheses. *BioMed Research International*. 2018; 2018 Available from: doi: 10.1155/2018/9634184 Available from:

<https://www.ncbi.nlm.nih.gov/pmc/articles/PMC6193342/> [Accessed May 28, 2020].

(14) O’Keeffe B. Prosthetic rehabilitation of the upper limb amputee. *Indian Journal of Plastic Surgery : Official Publication of the Association of Plastic Surgeons of India*. 2011; 44 (2): 246-252. Available from: doi: 10.4103/0970-0358.85346 Available from:

<https://www.ncbi.nlm.nih.gov/pmc/articles/PMC3193637/> [Accessed May 28, 2020].

(15) *bebionic hand*. Available from: <https://www.ottobockus.com/prosthetics/upper-limb-prosthetics/solution-overview/bebionic-hand/> [Accessed May 28, 2020].

(16) Ovadia SA, Askari M. Upper Extremity Amputations and Prosthetics. *Seminars in Plastic Surgery*. 2015; 29 (1): 55-61. Available from: doi: 10.1055/s-0035-1544171 Available from:

<https://www.ncbi.nlm.nih.gov/pmc/articles/PMC4317270/> [Accessed May 28, 2020].

(17) Sang Y, Li X, Luo Y. Biomechanical design considerations for transradial prosthetic interface: A review: *Proceedings of the Institution of Mechanical Engineers, Part H: Journal of Engineering in Medicine*. 2016; Available from: doi: 10.1177/0954411915624452 Available from:

<https://journals.sagepub.com/doi/10.1177/0954411915624452> [Accessed May 28, 2020].

(18) Ibitoye MO, Hamzaid NA, Zuniga JM, Abdul Wahab AK. Clinical biomechanics. *Clinical biomechanics*. 1986; 29 (6): 691-704. Available from:

<http://www.sciencedirect.com/science/article/pii/S0268003314000850> .

(19) Krueger E, Scheeren EM, Nogueira-Neto GN, Button, Vera Lúcia da Silveira Nantes, Nohama P. Advances and perspectives of mechanomyography. *Revista Brasileira de Engenharia Biomédica*. 2014; 30 (4): 384-401. Available from: doi: 10.1590/1517-3151.0541 Available from:

[http://www.scielo.br/scielo.php?script=sci\\_abstract&pid=S1517-31512014000400009&lng=en&nrm=iso&tlng=en](http://www.scielo.br/scielo.php?script=sci_abstract&pid=S1517-31512014000400009&lng=en&nrm=iso&tlng=en) [Accessed May 28, 2020].

(20) Tarata MT. Mechanomyography versus Electromyography, in monitoring the muscular fatigue. *BioMedical Engineering OnLine*. 2003; 2 3. Available from: doi: 10.1186/1475-925X-2-3 Available from:

<https://www.ncbi.nlm.nih.gov/pmc/articles/PMC443861/> [Accessed May 28, 2020].

(21) Ghapanchizadeh H, Ahmad SA, Ishak AJ, Al-quraishi MS. Review of surface electrode placement for recording electromyography signals. *Biomedical Research*. 2017; 0 (0): Available from:



<https://www.alliedacademies.org/abstract/review-of-surface-electrode-placement-for-recording-electromyography-signals-6117.html> [Accessed May 28, 2020].

(22) Ray GC, Guha SK. Equivalent Electrical Representation of the Sweat Layer and Gain Compensation of the EMG Amplifier. *IEEE Transactions on Biomedical Engineering*. 1983; BME-30 (2): 130-132. Available from: doi: 10.1109/TBME.1983.325209 [Accessed May 28, 2020].

(23) Woodward RB, Stokes MJ, Shefelbine SJ, Vaidyanathan R. Segmenting Mechanomyography Measures of Muscle Activity Phases Using Inertial Data. *Scientific Reports*. 2019; 9 (1): 1-10. Available from: doi: 10.1038/s41598-019-41860-4 Available from: <https://www.nature.com/articles/s41598-019-41860-4> [Accessed May 28, 2020].

(24) Wilson S, Vaidyanathan R. Upper-limb prosthetic control using wearable multichannel mechanomyography. *IEEE ... International Conference on Rehabilitation Robotics: [proceedings]*. 2017; 2017 1293-1298. Available from: doi: 10.1109/ICORR.2017.8009427 [Accessed May 28, 2020].

(25) Jones Charles, Puszet B, Bell E, Seddon Deane Z. *Group 19 Project Quality Plan*. London: Unpublished. 2019.

(26) Jones C, Puszet B, Bell E, Seddon Deane Z. *Group 19 Project Progress Report*. London: Unpublished. 2020.

(27) ASTM International. *ASTM C1055 Standard Guide for Heated System Surface Conditions that Produce Burn Injuries*. Available from: <http://www.astm.org/cgi-bin/resolver.cgi?C1055-20>.

(28) MatWeb L. *MatWeb Material Property Data*. Available from: <http://www.matweb.com/>.

(29) Backyard Brains. *Flexion and Extension: Record Your Antagonistic Muscles*. Available from: <https://backyardbrains.com/experiments/muscle2chspikerbox>.

(30) Hogan N, Mann RW. Myoelectric signal processing: optimal estimation applied to electromyography--Part I: derivation of the optimal myoprocessor. *IEEE transactions on bio-medical engineering*. 1980; 27 (7): 382-395. Available from: doi: 10.1109/tbme.1980.326652 [Accessed May 28, 2020].

(31) Hogan N, Mann RW. Myoelectric signal processing: optimal estimation applied to electromyography--Part II: experimental demonstration of optimal myoprocessor performance. *IEEE transactions on bio-medical engineering*. 1980; 27 (7): 396-410. Available from: doi: 10.1109/TBME.1980.326653 [Accessed May 28, 2020].

(32) Arduino. *Arduino Programming Language*. 2020.

(33) Posatskiy AO, Chau T. Design and evaluation of a novel microphone-based mechanomyography sensor with cylindrical and conical acoustic chambers. *Medical Engineering and Physics*. 2011; 34 (8): 1184-1190. Available from: doi: 10.1016/j.medengphy.2011.12.007 Available from: <https://www.clinicalkey.es/playcontent/1-s2.0-S1350453311003213>.

(34) Woodward RB, Shefelbine SJ, Vaidyanathan R. Pervasive Monitoring of Motion and Muscle Activation: Inertial and Mechanomyography Fusion. *IEEE/ASME Transactions on Mechatronics*. 2017; 22 (5): 2022-2033. Available from: doi: 10.1109/TMECH.2017.2715163 [Accessed May 28, 2020].



- (35) McCue TJ. *Wohlers Report 2018: 3D Printer Industry Tops \$7 Billion*. 2018.
- (36) E-NABLE. *Enabling the Future*. Available from: <https://enablingthefuture.org/>.
- (37) 3D Insider. *The 9 Different Types of 3D printers*. Available from: <https://3dinsider.com/3d-printer-types/>.
- (38) Llop-Harillo I, Pérez-González A, Starke J, Asfour T. Robotics and autonomous systems. 2019; 121 103259. Available from: <http://www.sciencedirect.com/science/journal/09218890> .
- (39) Matt. *Average Hand Size for Men, Women and Children*. Available from: <https://www.theaveragebody.com/average-hand-size/>.
- (40) Cordella F, Ciancio AL, Sacchetti R, Davalli A, Cutti AG, Guglielmelli E, et al. Literature Review on Needs of Upper Limb Prosthesis Users. *Frontiers in Neuroscience*. 2016; 10 Available from: doi: 10.3389/fnins.2016.00209 Available from: <https://www.frontiersin.org/articles/10.3389/fnins.2016.00209/full> [Accessed May 28, 2020].

